Republic of Iraq
Ministry of Higher Education
and Scientific Research
University of Anbar
College of Engineering
Mechanical Engineering Department

Hydraulic-Thermal Performance of a Double Pipe Heat Exchanger Filled with Annular Metal Foam

A Thesis
Submitted to the Council of the College of Engineering - University of Anbar in Partial Fulfillment for the Requirements of the Master Degree of Science in Mechanical Engineering

By

Thaer Hameed Farhan
(B.Sc. in Mechanical Engineering – 1999)

Supervised by

Asst. Prof. Dr. Obaid Talak Fadhil

Asst. Prof. Dr. Hamdi Emaduldeen Ahmed

1443 **2021**

Supervisor's Certification

I certify that this thesis entitled " ***Hydraulic-Thermal Performance of a Double Pipe Heat Exchanger Filled with Annular Metal Foam***" was prepared by "***Thaer Hameed Farhan***" under our supervision in the Mechanical Engineering Department of the University of Anbar as a partial fulfillment of the requirements for the degree of Master in Mechanical Engineering

Signature

Name: Asst. Prof. Dr. Obaid Talak Fadhil

Date: / / 2021

Signature

Name: Asst. Prof. Dr. Hamdi Emaduldeen Ahmed

Date: / / 2021

In view of the available recommendation, I forward this thesis for debate by the examining committee.

Signature

Name: Asst. Prof. Dr. Mazin Yaseen Abbood

Head of Mechanical Engineering Department

Date: / / 2021

Linguist Certification

This is to certify that I have read the thesis titled "***Hydraulic-Thermal Performance of a Double Pipe Heat Exchanger Filled with Annular Metal Foam***" and corrected any grammatical mistake I found. The thesis is therefore qualified for debate as far as language is concerned.

Signature

Name:

Date: / / 2021

Examination Committee Certification

We certify that we have read the thesis titled "***Hydraulic-Thermal Performance of a Double Pipe Heat Exchanger Filled with Annular Metal Foam"*** and as examining committee examined the student " in relation to all aspects of this thesis. In our opinion, it meets the standards of a thesis for the degree of Master (M.Sc.) in Mechanical Engineering.

Signature:
Asst. Prof. Dr Saad Mohammed Jalil
Date: / / 2021
(Chairman)

Signature:
Asst. Prof. Dr.Ammar Ali Farhan
Date: / / 2021
(Member)

Signature:
Lecturer Dr. Mohammed Ghanem Jehad
Date: / / 2021
(Member)

Signature:
Asst. Prof. Dr. Obaid Talak Fadhil
Date: / / 2021
(Member and supervisor)

Signature:
Asst. Prof. Dr. Hamdi Emadudeen Ahmed
Date: / / 2021
(Member and supervisor)

Approval of The College of Engineering

Signature
Asst. Prof. Dr. Mazin Yaseen Abbood
(Head of Mechanical Engineering Department)
Date: / / 2021

Signature
Asst. Prof. Dr. Ameer Abdurrahman Hilal
(Dean of Engineering College)
Date: / / 2021

Declaration

I hereby declare that this thesis, submitted to mechanical engineering department at Anbar University as a requirement for the master degree, has not been submitted as an exercise for similar degree at any other universities. I also on this work that is qualified here is entirely my own except for excerpts and summaries whose sources are congruently cited in the references.

Thaer Hameed Farhan

2021

Acknowledgments

Thanks to Allah for his entire blessing who gave me the support, power, and patience.

I would like to express my sincere gratitude to my supervisors (***Asst. Prof. Dr. Obaid Talak Fadhil*** and ***Asst. Prof. Dr. Hamdi Emaduldeen Ahmed)*** for their continuous support during my M.Sc. study.

I also like to express my gratitude to the head and staff of the Mechanical Engineering Department, University of Anbar especially ***Asst. Prof. Dr. Mazin Yaseen Abbood*** the head of the department for his encouragement.

I would like to thank my dear father, my compassionate mother, my wife, my brothers and sisters, and everyone who provided me with support and advice.

Abstract

This study is an experimental attempt to improve the performance of a double-pipe type heat exchanger, by placing copper-metal foam with various configurations inside an annular space between the inner pipe and the outer pipe of the heat exchanger. The test section consists of two concentric pipes with a length of 500 mm, the inner pipe is made of copper with nominal diameter of 18 mm, and the outer pipe is 42 mm in diameter and is made of plastic. A copper metal foam with 15 pore per inch, and a porosity of 0.95 was used.

Air was used as a working fluid in both hot and cold streams. A wide range of cold air flow rate was covered, namely; (3, 6, 12, 18, 24, 30, and 36) m^3/h, which corresponds to Reynolds number ranged from 2811 to 31,335. Whereas the hot air flow rate was kept constant at 3 m^3/h. The temperature difference between the inlet hot air and inlet cold air was adopted to be (20°C, 30°C, 40°C, and 50°C). The results reveal that the heat transfer, pressure drop and effectiveness depend on the configuration of the metal foam. Also, the heat transfer rate of the heat exchanger with the metal foam for all the arrangements is the greater than the smooth heat exchanger. The friction factor is higher when the metal foam is used than the smooth heat exchanger. The friction factor is found to be affected strongly by the metal foam configuration more than metal foam amount. It also decreases with increasing Reynolds numbers. The results also show that the best performance evaluation criteria is 1.62 for case 7 at lowest Reynolds number 2800.

List of Contents

List of Tables

List of Figures

Nomenclatures

Symbol	Description	Units
A_i	Inner Surface area of copper pipe	m^2
A_o	Outer Surface area of copper pipe	m^2
A_c	Cross section area of annular gap	m^2
AR	Air ratio	-----
c_p	Specific heat at constant pressure	kJ/kg. °C
d_i	Inner diameter of copper pipe	M
d_o	Outer diameter of copper pipe	M
D_i	Internal diameter of polyvinyl chloride PVC pipe	M
D_O	Diameter of outer PVC pipe	M
D_h	Hydraulic diameter	M
E	heat exchanger effectiveness	----
F	Friction factor	-------
h_o	Convection heat transfer coefficient with the cold air	W/m^2 K
h_i	Convection heat transfer coefficient with the hot air	W/m^2 K
K	Thermal conductivity of fluid	W/m K
$\dot{m}$	Air Mass flow rate	kg/s
ΔP	Pressure drop across the heat exchanger	Pa
Q	Heat transfer rate	W
U	Fluid Velocity	m/s
$\dot{V}$	Air volumetric rate	m^3/s
T	Temperature	°C
Re	Reynolds number	-------
$T_{h\ ave}$	Average hot air temperature	°C
T_{hi}	Inlet hot air temperature	°C
T_{ho}	Outlet hot air temperature	°C
$T_{c\ ave}$	average cold air temperature	°C
T_{ci}	Inlet cold air temperature	°C
T_{co}	Outlet cold air temperature	°C

$T_{s_{ave}}$	average surface temperature of copper pipe	°C
Nu_{MF}	Nusselt number with metal foam	----
Nu_s	Nusselt number without metal foam (smooth)	----
f_{mf}	Friction factor with metal foam	----
f_s	Friction factor without metal foam (smooth)	----
Greek symbols		
ρ	Air Density	kg /m^3
μ	Air Viscosity	N.s / m^2
ε	porosity	-----
Abbreviations		
PPI	Pores Per Inch	
LPM	Liter per minute	
PEC	Performance Evaluation Criteria	
MF	Metal Foam	
PVC	Polyvinyl Chloride	
r.p.m	Revolution per minute	

CHAPTER ONE
INTRODUCTION

1.1 Background

The heat exchanger is a device that allows heat exchange between two fluids of different temperatures without contact. It is used in various industrial and engineering applications electrical stations, thermal power plants, chemical processing plants and petrochemical industries, where the heat exchanger is located between two circuits of the main and secondary water [1].

The share of heat exchangers industries is a great interest by companies and researchers for the purpose of increasing its performance by using one of the performance improvement techniques, whether by the method of their design or methods of fluid flow in them or through the use of wires, washers, fins and metal foam [2].

Therefore, enhancing the thermal performance of heat exchange affects directly on energy, material and cost savings. Heat exchangers are normally classified by transfer according to Phase, fluid numbers, compactness of the surface, features of the building, flow structures, and heat transfer facilities. A heat exchanger design restores the largest possible amount of heat from the exhaust gases to reduce costs and protect the environment [3].

1.2 Double Pipe Heat Exchanger

The heat exchanger job is to transfer heat between two fluids of different temperatures that are separated by a solid wall. The difference in temperatures of the two fluids causes heat to be transferred from the hot fluid to the cold fluid, where the heat is transferred by the three

known methods, which are conduction, convection, and radiation. The amount of radiation is less than convection and conduction in heat transfer in heat exchangers and can be neglected in many cases [4].

Heat is transferred from the hot fluid to the wall of the pipe by convection, and then by conduction through the pipe wall, and then by convection from the wall of the pipe to the cold fluid. The wall of the pipe is usually of a small thickness, metal with high thermal conductivity, to increase the amount of heat transfer between the two fluids [5].

One of the simplest types of heat exchangers is the two-pipe heat exchanger, and it was called by this name because it consists of two concentric pipes, where one fluid flows in the inner pipe, and the other fluid flows into the annular space between the two pipes. The double-pipe heat exchanger is classified into two types according to the direction of flow of the hot fluid and the cold fluid as shown in Fig. 1.1. They are the parallel-flow heat exchanger, where both fluids flow in the same direction, and the counter-flow heat exchanger, where the two fluids flow in opposite directions [6].

In a double-pipe heat exchanger, the hot fluid passes through the inner pipe, while the cold fluid passes through the annular space between the two pipes.

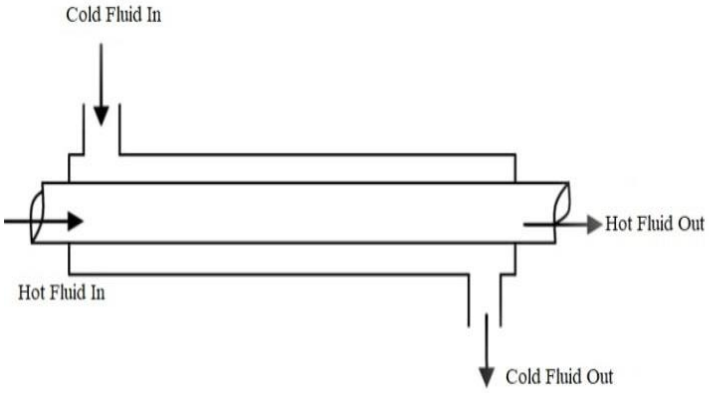

(a)

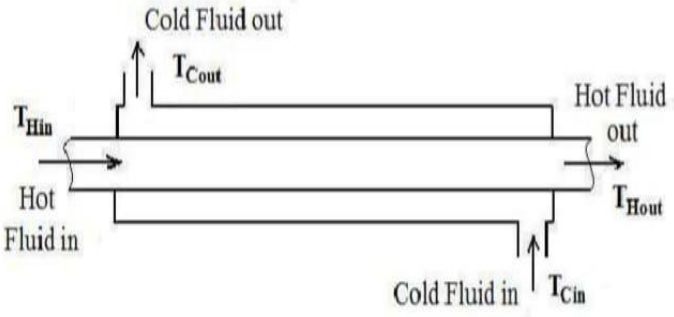

(b)

Figure 1.1 Double-pipe heat exchanger (a) parallel-flow, (b) counter-flow [6].

1.3 Techniques of Heat Transfer Enhancement

There are several techniques used to improve the convection heat transfer in general, and in heat exchangers in particular. All these techniques depend on the principle of increasing the convection heat transfer coefficient, increasing the heat transfer surface area, or increasing both of them.

An increase in the convection heat transfer coefficient can occur as a result of an increase in the turbulence of the fluid flow, and this can happen by increasing the roughness of the surface of the duct in contact

with fluid, installing fins, spiral wires, twisted tapes [3], or using one of the types of porous materials such as metal foam. Increasing the heat transfer area can be done by making grooves inside the duct, placing fins or ribs on the inner surface of the duct [3], or inserting metal foam inside the duct can increase the heat transfer area.

The using of metal foam for improving heat transfer is considered one of the modern techniques to provide these materials at an affordable price in addition to their other advantages, which could increase the area of heat transfer. It should be Notice that all the previous heat transfer improvement techniques result in a loss of fluid pressure, and thus increase the power consumed to pump the fluid [7].

1.4 Porous Medium

The shape of the porous medium is solid arrays that contain pores (spaces) in order to allow the fluid to pass through them. The most important type of porous medium is porous metal foams which are used in many heat transfer applications and have many different shapes and specifications [8].

It has many features and unique specifications, especially when compared with other materials. High thermal conductivity has emerged as an important method of heat transfer improvement. The ratio of surface area to volume and extreme flow mixing also porous media characterized by as it has great strength, high thermal conductivity, lightweight, ease of manufacture and less cost. [8].

1.4.1 Metal Foam (MF)

Metal foam is a porous material that usually made of solid metals, it is a mixture of gas or pores and metal. It is a spongy cluster structure and because the metal foam contains a high percentage of pores, it allows

gases and liquids to pass through them. There are two types of metal foam the first type is closed pores, and the second type is the open pores. Metal foam are nowadays made of aluminum, copper, zinc, nickel, titanium, and magnesium. Many modern engineering research has focused on the use of materials that are lightweight and can save energy, and metal foam is one of these materials [9].

The metal foam can be by many physical and mechanical specifications such as ;effective thermal conductivity (0 – 10 W/m. K), high fluid-solid interfacial area (i.e. high lightweight, low fabrication cost , high strength and rigidity, long flow path through the porous matrix, and fluid mixing which enhances the convection heat transfer surface area per volume, 500–10,000 m^2/ m^3), and high thermal energy absorption [8].

The most important of those improvements is to enhance the effective thermal performance technique which was used for effective heat exchangers that were made and the focus of this research the use of metal foam. The use of metal foam because of many features that researchers use in double pipe heat exchangers, their porosity of MF, which allows fluids to penetrate easily, it was increasing the surface area of contact and enhancement of fluids mixing, which allows the fluid to conduct a path winding. High mechanical strength, low production cost, ease of use, and high thermal conductivity are the main characteristic of porous material [10].

There are many applications for open-cell metal foams such as power plants, industrial plants, cooling machines, heat exchangers, separation and filtration, and purification of water [11].

One of the important mechanical properties of the MF is the Pore Per Inch (PPI) which is defined as the number of pores in one linear inch as shown in Fig. (1.2). The normal PPI range is from 10 to 80 PPI, whereas

10 PPI has large cells and is fully open, while 80PPI has smaller cells and provides a higher pressure drop [8].

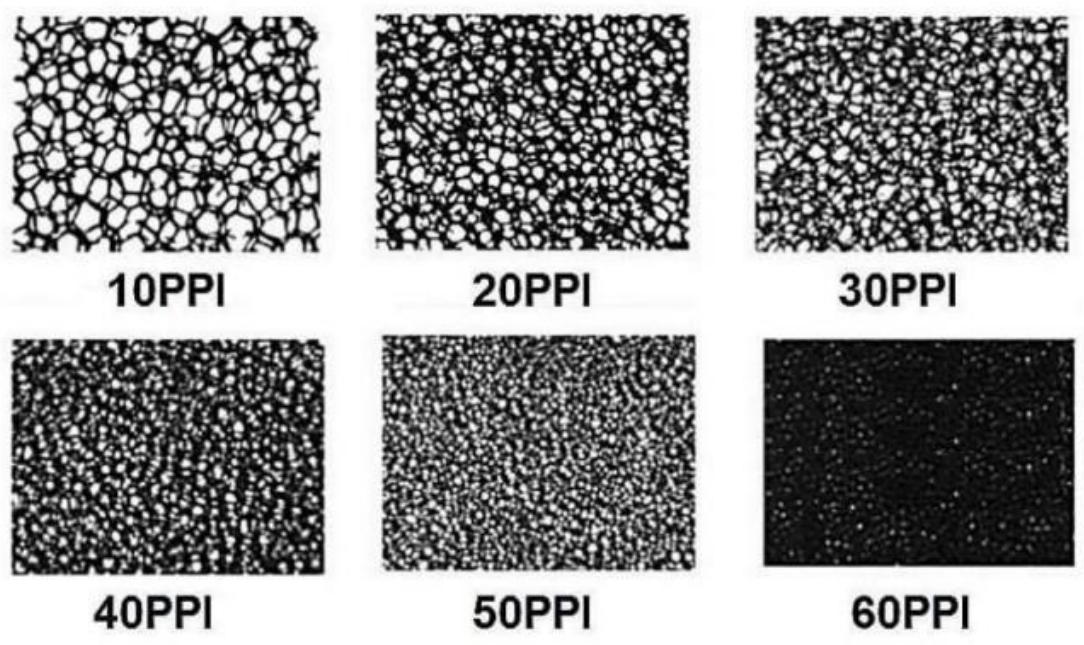

Figure 1.2 Metal Foams having different PPI [11]

Another major property of metal foam is the porosity which is denoted by (ε). It can be defined as the ratio of voids to the total volume of MF as shown in Fig. (1.3) [11].

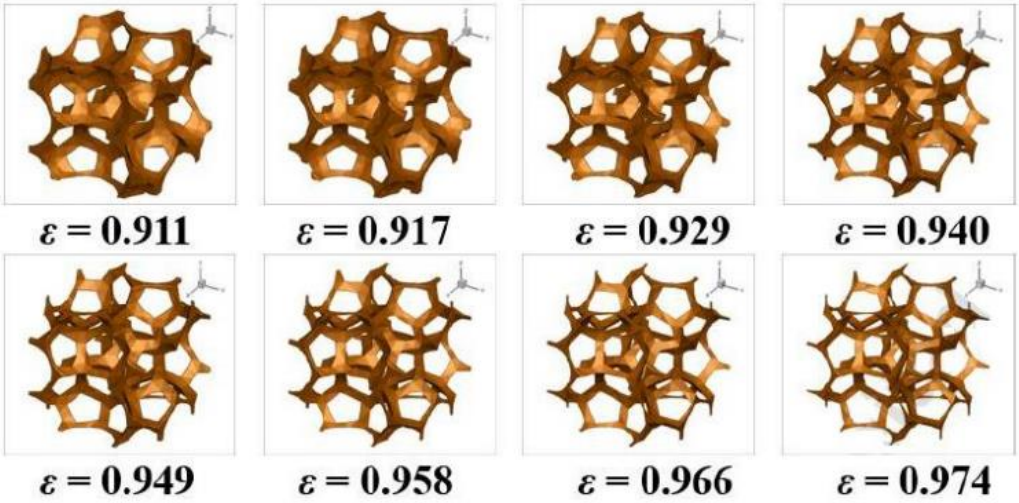

(a)

Figure 1.3 Metal foam porosity (ε) [11].

1.5 Problem Statement

The heat transfer rates in double-pipe heat exchangers are limited by the thermal conductivity of the wall, fluid flow direction, type of flow regime, heat transfer surface area, fluid mixing, as well as thermo physical properties of the coolant liquid. In order to enhance the convection heat transfer coefficient, passive techniques can be applied without additional expensive costs or external forces. Metal foam can be used in several configurations, to fill the annular gap partially or completely [12].

The low thermal conductivity of the air, low convection heat transfer coefficient of the smooth rings, the increased pressure drop due to the extended solid surfaces, and the additional weight encourage the authors to use different techniques to improve the overall performance of the heat exchangers.

The main job of the present work is to enhance the heat transfer of a double pipe heat exchanger by inserting metal foam in different

configurations in the annular space. From the view point of the proposal makers, there is no publication that has studied the effect of the MF arrangement and configuration in the double pipe heat exchanger yet.

1.6 Objectives

The objectives of the current study can be summarized as follows:

1- Investigate the effect of full filled annulus with metal foam on the heat transfer and pressure drop. Study the effect of partially filled annulus with metal foam on the Performance Evaluation Criteria.

2-Explore the influence of different configurations of the metal foam ,Examine the continuous and periodic filling of the annulus with metal foam on the Performance Evaluation Criteria.

1.7 Outline of the thesis

The dissertation is divided into five chapters. Each chapter is briefly explained as follows:

Chapter One: Describes the general background for the double pipe heat exchanger, techniques of heat transfer enhancement, porous medium, problem statement, objectives of the current study and outline of the dissertation.

Chapter Two: This chapter presents the numerical and experimental studies that have been conducted for the purpose of improving heat transfer of the heat exchangers.

Chapter Three: Includes a description of the device used in the study with a definition of each part, the procedure of the work and data collecting with an explanation of the calibration of the devices, the equation of variables calculations, and range of variables.

Chapter Four: presents the results with thorough interpretation and analysis. The effect of metal foam arrangement on the local wall temperature, local and average Nusselt number, effectiveness, pressure drop, friction factor, and thermal hydraulic performance are presented.

Chapter Five: summarizes the current experimental work and recommendations for future works.

CHAPTER TWO
LITERATURE REVIEW

2.1 Introduction

This chapter Include a review of the literature, which is concerned with heat exchangers and in particular for double pipe heat exchangers. Studies reported in the literature review can be divided into three sections; experimental studies, numerical studies, experimental and numerical studies.

2.2 Experimental Studies

Hamzah and Nima [13] investigated the effect of inserting copper metal foam fins (MFF) having (40 PPI) with an inclination angle of (30°) with the flow direction on the heat transfer and pressure drop in a double-pipe heat exchanger. The MFF was inserted inside the annular gap on the outer surface of the inner copper cylinder. The Reynolds number of cold air was ranged from 616 to 2343, while the hot water flow rate was 2 L/min with inlet water temperature of (80°C, 85°C, and 90 °C). Parallel and counter flows were explored and compared with and without the MFF. It was found that cold air when Reynolds number increased the average heat transfer coefficient and the average Nusselt number increased. The high thermal enhancement was obtained in the case of MFF insertion for counter-flow mode. They claimed that there was a small increase in the pressure drop when MFF was used. The convection heat transfer coefficient was observed to increase with increasing Re.

Abbas et al. [14] carried out an investigation to improve the heat transfer in a double-pipe heat exchanger using water. Several fin shapes were introduced (semicircular fin, a pipe with circular fin, and a pipe with

spiral fin) with smooth heat exchanger. The fluid flows inside the internal cylinder was either cold or hot. The results showed that the highest heat transfers in the circular finned pipe when the hot water flows inside the pipe. The heat transfer increased by 250% for counter flow and 165% for parallel flow.

Maid et al. [15] studied the heat transfer in counter-flow a double pipe heat exchanger using metal pads. Authors evaluated the effect of metal pads on heat exchanger efficiency, heat transfer coefficient, and pressure drop. Cold water was flowed into the gap and hot water was flowed into the inner pipe. The hot water flow rate was between (0.066–0.198) kg/s, (4862< Re < 14,633) the cold-water flow was constant at (0.197) kg/s, Re = 2912 the cold-water temperature was (18^{o}C), and the hot water temperature was (43^{o}C). It was noticed that the most important factors that affect the axial distribution of temperature, efficiency, heat transfer coefficient, and pressure drop were the mass flow rate and the use of metal pads.

Mishra and Nayak [16] studied the heat transfer in a double concentric pipe heat exchanger with and without triangular baffles for parallel and contrary flow. The diameter ratio was 3.17 and a length of 2438 mm. It was observed that the efficacy increased with the rise of the flow rate of cold fluid. The average effectiveness improved, when the pitch of baffles was 100 and 50 mm, the average effectiveness was enhanced at 1.42 and 1.622 time in Parallel-flow and 1.34 and 1.62 time in counter-flow that Smooth pipe, respectively. It was concluded that the heat exchanger that contains triangular baffled has higher performance than the smooth heat exchanger.

Nawaz et al. [17] proved that increasing the heat transfer by using open-cell metal aluminum framing using an air tunnel as shown in Fig. (2.1).

The heat transfer was increased due to the mixing of the fluid and the increase in the surface area, associated with high pressure drop when the MF was used. Foams with less porosity increase the pressure drop and increase the heat transfer rate. Fin height could be changed to reduce the pressure drop. They found that the best efficiency was with metal foams compared to regular fins.

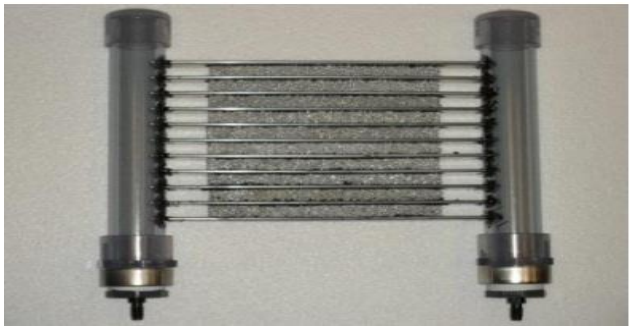

Figure 0.1 Flat pipe heat exchanger metal foam[17].

Govindani [2] fabricated a double-pipe heat exchanger with a rotor assembly strand for increasing turbulence in the fluid flow where the water was used as a coolant. Reynolds number was ranged between 3000 and 15,000. They observed higher turbulence in the flow of the fluid and higher heat transfer compared to the empty pipe as shown in Fig. (2.2).

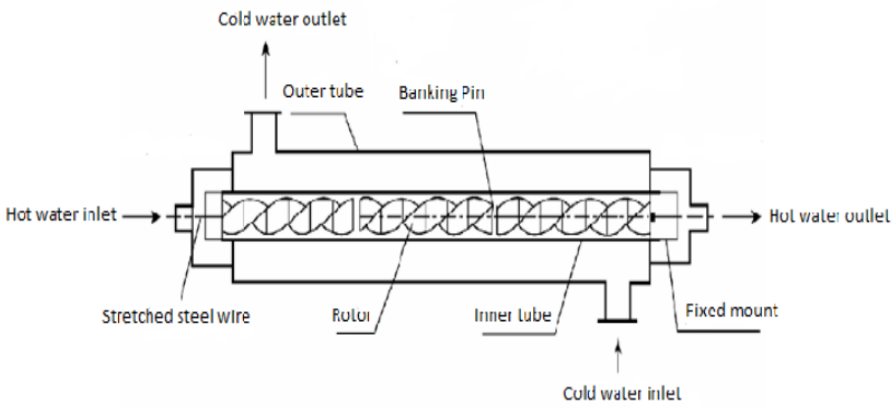

Thejaraju et al. [1] studied the effect of inserting Para-Winglet Tape on the thermal behavior of the heat exchanger with the range of Reynolds

number of (6000–30,000). Three types of tape were used with different angles. It was found that when semi-winged tape was used an increase in the turbulent kinetic energy was obtained causing an increase in the heat transfer. The highest value of the Nusselt number was obtained at the highest Reynolds number while the friction factor decreased by increasing the Reynolds number.

Sertkaya et al. [18] The use 6 an heat exchanger . The first three heat exchanger are made of aluminum with fins of metal foam. Fin spacing are 1.6, 3.2, 4.8 mm. The other three are made of aluminum with open-cell foam (10, 20, and 30 ppi) used by Reynolds range ($5\times10^3 – 9\times10^4$). They concluded that the efficiency of the exchanger decreases and the pressure increases with the increase in the velocity of refrigerant increased and that the higher efficiency is at the lower Reynolds numbers. Fins made of aluminum are more efficient than those made of aluminum foam.

Sheikholeslami et al. [19] fabricated double pipe heat exchanger in which hot water and cold air were used in the experiment as shown in Fig. (2.3). A Typical Circular Ring (TCR) and a Perforated Circular Ring (PCR) were used inside the annular pipe; air passed through the annular pipe and the water passed through the inner pipe. Reynolds number was adopted from (6000–12,000) and the number of holes was (0, 2, 4, 8). It has been shown that the use of (CRS) could improve heat transfer greater than (PCRS) while the friction factor was less for PCRS. The Nusselt number increased with increasing Reynolds number and the number of holes. Whereas the friction factor decreased with increasing Reynolds number and decreasing the number of holes.

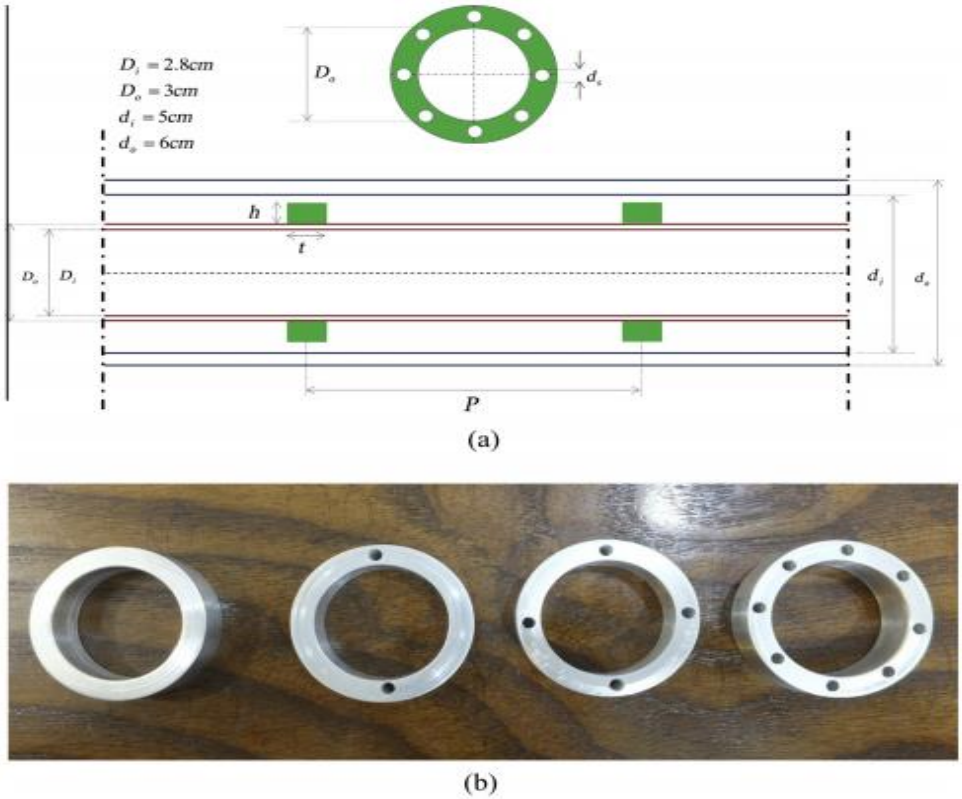

Figure 0.3 (a) Test section; (b) typical circular-ring (TCR) and perforated circular-ring (PCR) tabulators [19].

2.3 Numerical Studies

Targui and Kahalerras [4] studied the heat transfer and flow characteristics in a double-pipe heat exchanger by installing porous structures within the gap between the two pipes either on the outer surface of the inner pipe or on the inner surface of the outer pipe and on the outer surface of the inner pipe in an overlapping manner. The optimal thermal design was found at the utilization of the porous structures on the inner surface of the outer pipe and on the outer surface of the inner pipe. Also, the heat transfer rate was increased when the thickness of the porous structure increased and when the distances (pitch) were reduced heat.

Kahalerras and Targui. [20] studied the effect of using porous fins installed on the outer wall of the inner cylinder in a double-pipe heat

exchanger. The optimization was carried out by taking into consideration the effect of the fin height, fin spacing, and conductivity ratio. The rise in heat transfer was large by using porous fins, whereas their geometric shapes and the physical and thermal properties had evaluable effect on the improving of heat transfer. Researchers obtained an optimal heat transfer by optimizing the thermal conductivity ratio, fin spacing, and fin height.

Chen et al [21] simulated a double pipe heat exchanger with using metal foams with porosity (0.8–0.95) and pore density (5PPI–30PPI). The effect of flow direction, porosity, pore density, thermal conductivity on the efficiency, and pressure drop were included. They concluded that the heat transfer in the case of counter flow increased by 37.5% compared to the parallel flow and the maximum overall performance was at (15 PPI) and the performance was better in the case of using low porosity and low pore density on both sides of the inner pipe wall.

Rashidian and Tavakoli [12] studied the effect of using porous materials on the heat transfer in heat exchangers. They concluded that the efficiency of heat exchangers can be improved by using porous materials significantly.

Moghadasia et al. [22] examined the effect of porous media and Nanofluid, Darcy numbers and the porous thickness ratio on the heat transfer rate. PEC improved by enhancing the Darcy number. When the Darcy number decreases from 0.1 to 0.0001, the Nusselt number increased. Also, when the porosity increased and constant Darcy number, an increase in the pressure drop was seen.

Benmerkhi et al. [23] studied the forced convection flow in an oval foamed aluminum annulus with (20PPI) by using water as a coolant. The

inner cylinder was heated uniformly so that the temperature remains constant for the outer cylinder. They found that the convection reaches a development temperature that exceeds 40% of the length of the annulus compared to the empty annulus. The average Nusselt number was more than 5.88 times compared to the empty annulus. The Nusselt number increased with the increase of the Reynolds number.

Orihuela et al [10] studied the forced convection heat transfer of annulus filled with aluminum metal foam having 5PPI and 20PPI, and the flow rate was (20, 85, 150) L/min. The vertical annular temperature with the use of metal foam for the exchanger that the pressure drop is proportional to the length of the metal foam used. The airflow rate was more effective on the pressure drop than the pore density or the metal foam length that led to a higher heat transfer rate and a higher pressure drop with neglecting the size of the pores. Through their study, they found that the foam with 20PPI had better thermal performance than 5PPI when the airflow rate is 20LPM.

Jamarani et al. [24] studied the turbulent heat transfer in a double-pipe heat exchanger filled partially with metal foam as shown in Fig. (2.4) for improving the thermal performance, The inserting of porous materials led to an increase in heat transfer and the pressure drop compared to the heat exchanger without metal foam the higher PEC occurs in S=0.7andS=0.4(S= A_P $/A_i$)for configurations A and B, respectively

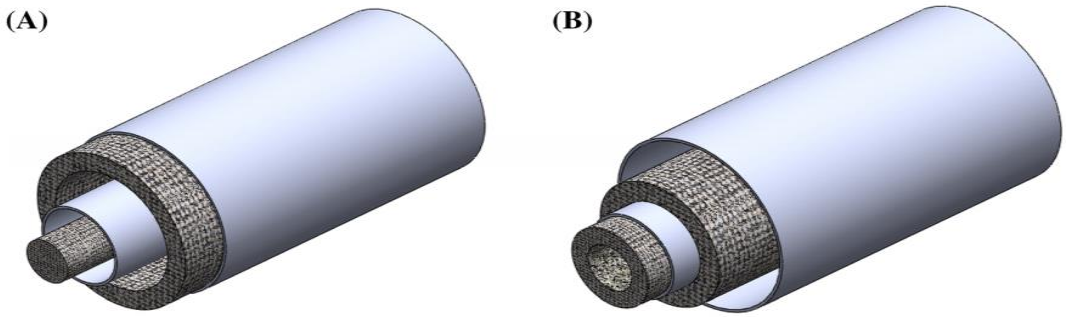

Figure 0.4 Schematic diagram of the double pipe heat exchanger (A) foam filled the center of inner cylinder and the inner surface of outer cylinder (B) foam filled of inner surface of inner cylinder and the outer surface of inner cylinder [24].

Chikh and Allouache [7] investigated the effects of the thickness of the porous substrate, its permeability, its thermal conductivity, and the difference in the inlet temperatures. They tried to reduce the entropy generation to find a compromise solution in an annular heat exchanger between improving heat transfer and reducing pressure drop. The porous insert with an optimum thickness (d_e) a substantial reduction in the pressure drop. For thin porous inserts not exceeded around 40 % of the annular gap, this heat transfer improvement was of considerable merit.

Nasser et al [5] used the metal rotating foam in a counter–flows, double- pipe heat exchanger for enhancing the heat transfer. They installed a layer of metal foam on the connecting surface between the two pipes in order to enhance the thermal conductivity across it. The heat exchanger was partly filled with a layer of metal foam with a high porosity and rotating coaxially. They demonstrated that it can further enhance heat transfer and save pumping energy compared to fully filled heat exchangers. The heat transfer can be greatly enhanced and the style considerations need to be taken carefully to prevent conflicts uneconomical optimization resulting from potential increases in the Pressure drop penalty.

Abbasi et al. [25] assessed the evaluation and development of shell-and-pipe heat exchanger shown in Fig.(2.5). They investigated the effect of the thickness of baffles, the number of baffles, and the angle of installation of the baffles. They reported that higher number of baffles provides higher heat transfer rate and higher pressure drop. They found that the best performance when ten baffles were used with an angle of 111.9º and baffles thickness of (16.69 mm). Authors also concluded that an exchanger could be designed to increase the heat transfer rate by 11.15% and decrease the pressure drop by 61.3% simultaneously. A higher number of baffles and lower baffle angles resulted in a higher rate of heat transfer, and a decrease in the pressure drop.

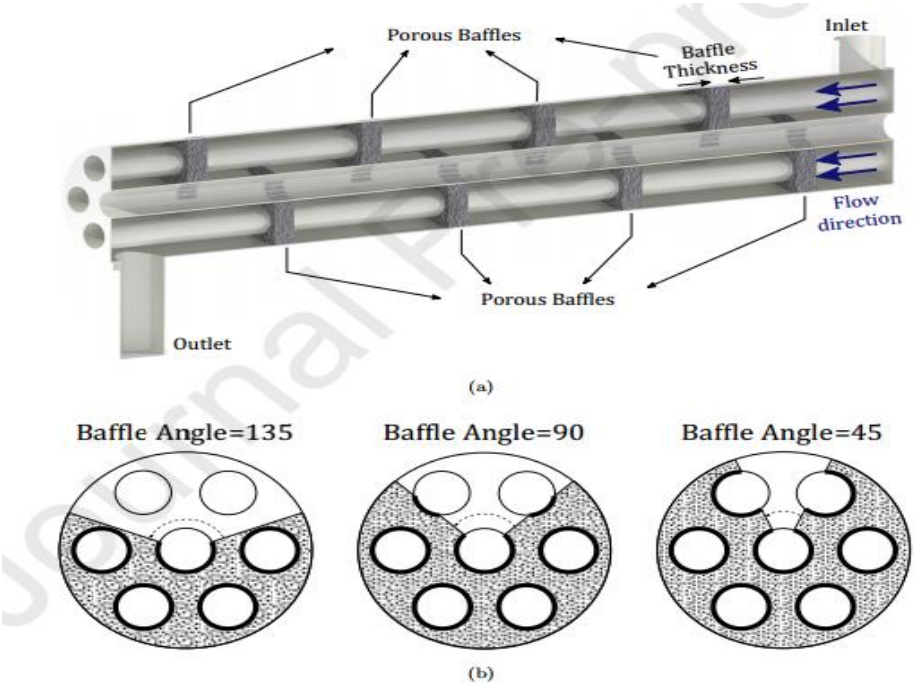

Figure 0.5 The schematics of the evaluated shell-tube heat exchanger. (a) 3D cross-section view, (b) Cross-section of porous baffles [25].

Odabaee and Hooman [26] studied the efficient heat exchangers with the use of metal foams by replacing the finned pipes in the cooled condensers. They tried to increase the heat transfer from a single-cylinder in cross-flow by enveloping a sheet of metal foam on the outer

surface of the channel. Heat exchangers with metal foam increased the efficiency from 2 to 6 times higher than the traditional design.

Ibrahim et al. [27] improved the transfer of latent heat in thermal energy storage systems by improving thermal conductivity by using porous materials. They concluded that the heat transfer could be improved either by increasing the thermal conductivity of the storage material phase change material or by increasing the heat transfer area of the storage system. They could enhance the heat transfer of the thermal storage system by using fins and extended pipes, and for by using high conductive materials such as porous media. Their study concluded that the use of fins was beneficial for the thermal performance of latent heat storage systems.

Xu et al. [28] verified numerically the behavior of a counter-flow double-pipe heat exchanger filled with metal foam as shown in Fig. (2.6). They concluded that effectiveness can be improved by reducing porosity and increasing pore density. They found that the pressure drop can be reduced by increasing the porosity or reducing the pore density. The porosity less than 0.9 and the pore density greater than 10PPI could have an efficiency of the heat exchanger greater than 0.8.

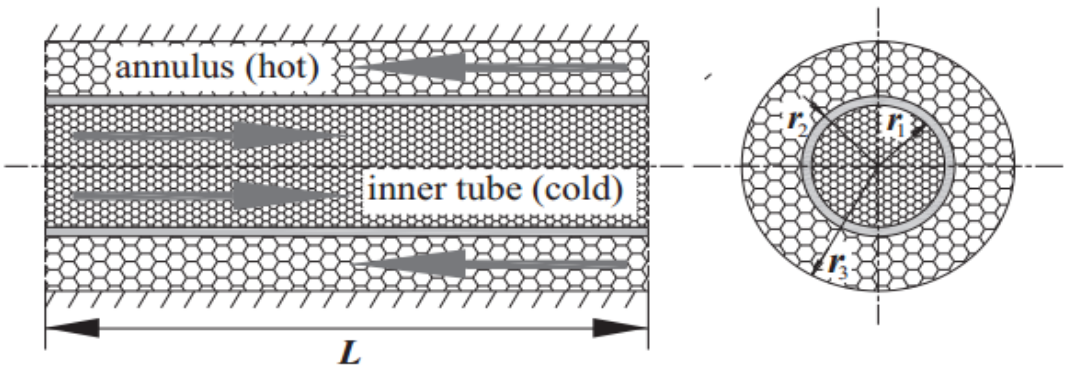

Figure 0.6 Schematic diagram of counter-flow double-pipe heat exchanger filled with metal foams [28].

Arasteh et al. [29] studied the heat transfer and fluid flow in a counter flow double-pipe heat exchanger as shown in Fig. (2.7). They obtained the rate heat transfer of 69%, overall heat transfer coefficient of 124%, efficiency of 9% and that the PEC of 1.36 when the metal foam was used in both streams, hot and cold in a partial configuration and periodically. They proved that optimally distributed and partitioned metal foams could enhance heat transfer more economically. Also, the inserting of metal foams in the same longitudinal locations in both pipes caused a higher heat transfer rate.

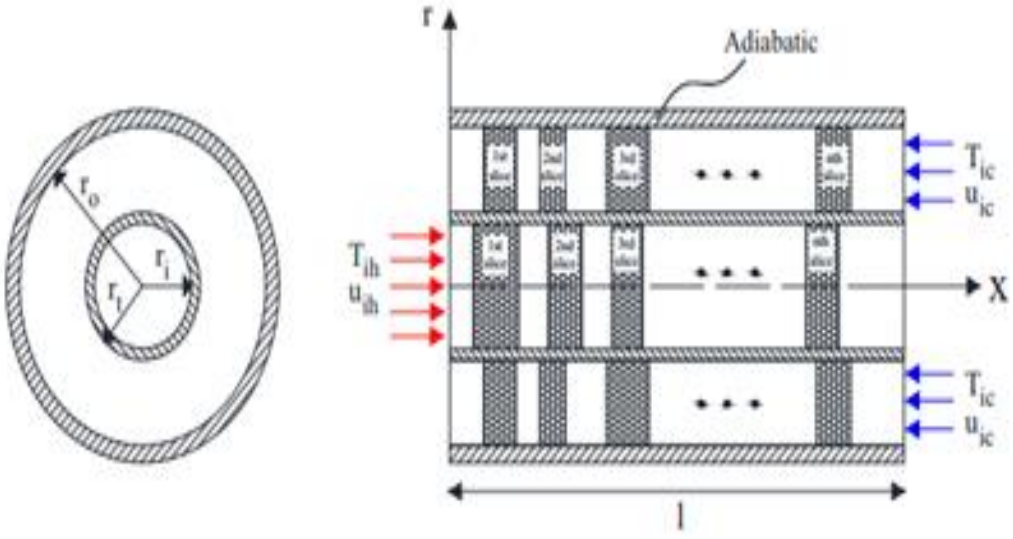

.

Figure 0.7 Schematic diagram of the double pipe heat exchanger with metal foam [29].

Zhao et al. [30] studied the forced convection heat transfer in a double pipe heat exchanger filled with high porosity metal foam. It was concluded that the thermal efficiency of their proposed design was higher than the ordinary heat exchanger particularly when the PPI increased and the porosity decreased. The effectiveness of the exchanger was increased as a function of the cross-section ratio of the flow and the pores density of the metal foam.

Targui and Kahalerras [35] studied the effect of pulsating flow and porous baffles on the thermal performance of the double pipe heat exchanger as shown in Fig. (2.8). The cold liquid flows in the gap between the two pipes while the hot liquid flows in the inner pipe. The use of the porous baffles and a pulsating flow could enhance the heat transfer and increased the thermal performance of the heat exchanger.

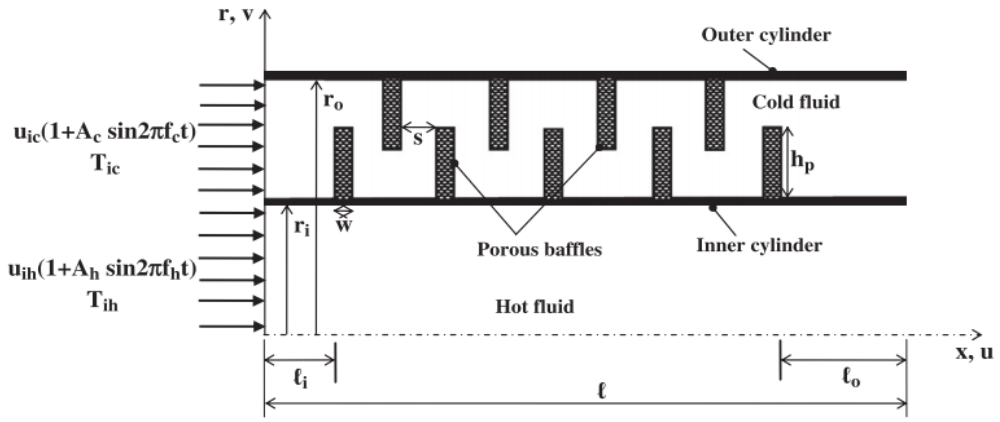

Figure 0.8 Physical domain of a double pipe heat exchanger with porous baffles [35].

2.4 Experimental And Numerical Studies

Zhao et al. [31] compared between a porous finned heat exchanger and a heat exchanger containing solid fins to find the best technique for recovering the lost heat from exhaust gas for engines as shown in Fig. (2.9). The Reynolds number was ranged from (5000–50,000). The results showed that the porous fins heat exchanger improved the heat transfer by 73.2–77.1%, decreased the pressure by 15.1%–18.5%, and reduced the weight of the heat exchanger by 90% at a porosity of 0.9. The performance evaluation factor was increased by 41%, compared to the traditional one.

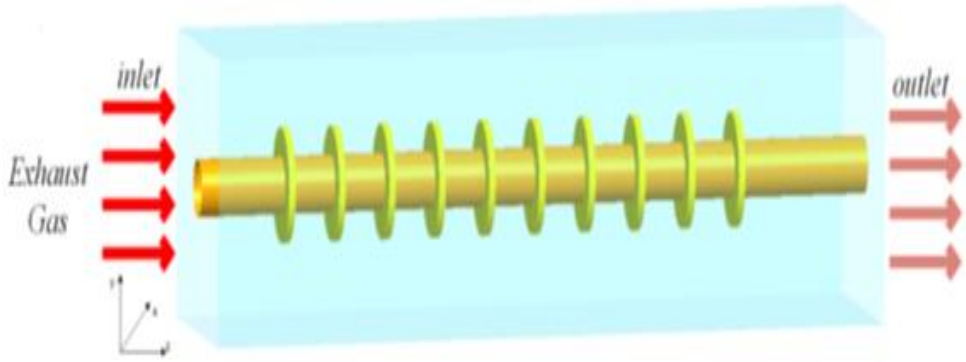

Figure 0.9 Schematic diagram of single-pipe heat exchanger with porous fins [31].

Pavel and Mohamad [32] studied the pressure drop and heat transfer by inserting the porous metal foam into the gap of annulus. The parameters of porosity, material diameter and thermal conductivity, as well as Reynolds number were investigated. It was found that the heat transfer rate was higher by using the porous materials at a reasonable expense of pressure drop as well.

Chen et al. [33] studied the effect of metal foam inserted in a double pipe heat exchangers on the heat transfer as shown in Fig. (2.10), and compared with the smooth one. The results obtained showed a significant increase in the heat transfer when using metal foam compared to ordinary heat exchanger associated high pressure drop.

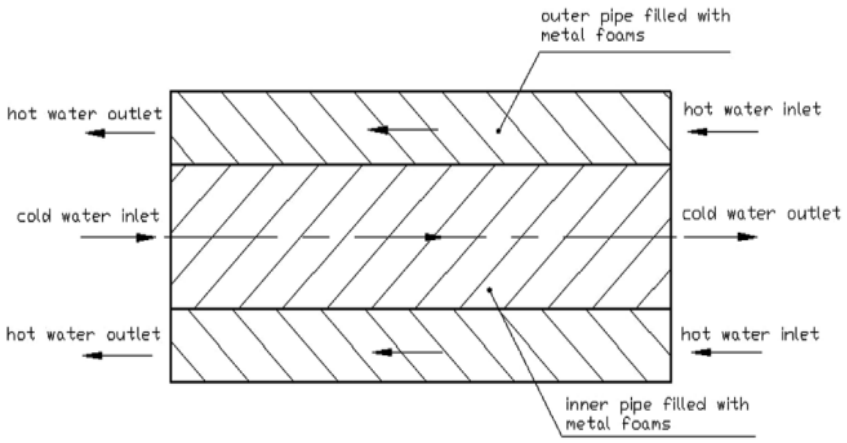

Figure 0.10 Schematic diagram of the cross sectional view of double-pipe heat exchanger filled with metal foams [33].

Alkam and Al-Nimr [34] studied a method to improve the performance of the double pipe heat exchanger as shown in Fig. (2.11). Using of porous substrates installed on the outer wall of the inner pipe, showed an improvement in the heat transfer by convection between the pipe wall and the fluid. The porous substrates also increased in the efficiency of the heat exchanger. They porous substrates could also increase in the pressure drop in the heat exchanger. Using an appropriate thickness of the substrates led to further improvement in the performance of the heat exchanger they studied.

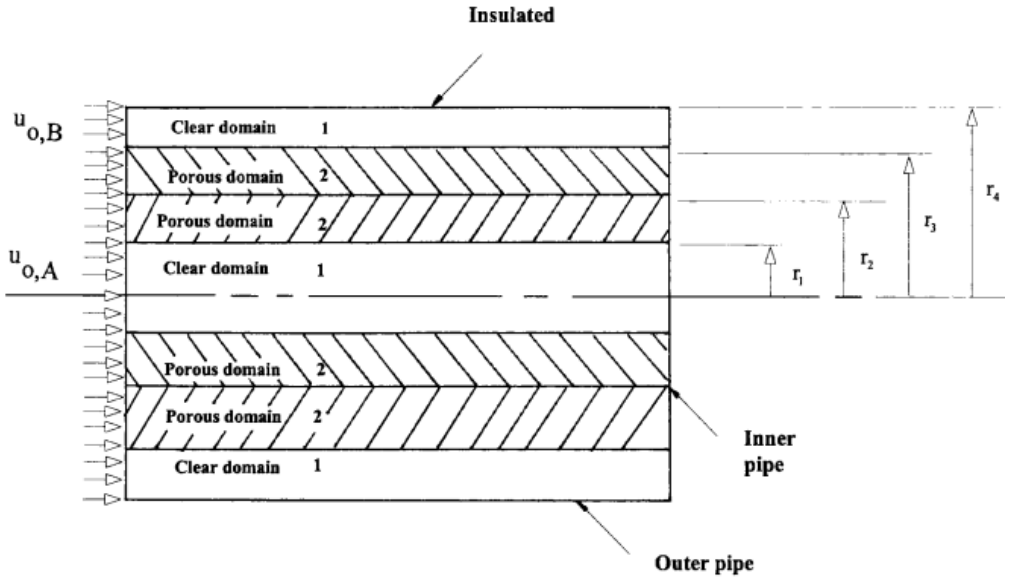

Figure 0.11 Schematic diagram of a double-pipe heat exchanger with porous substrates [34].

Table 0-1: Summary of the Numerical and Experimental Research Studies

Author	Study type	Relevant information	Key results
Hamzah and Nima [13]	experimental	MFF, copper(40PPI) Re_C= (616 to 2343) Water volumetric flow rate=2 L/min Water-air . air volumetric flow rate (5, 7, 9, 11, 13, 15, 17, 19 m^3/h	They claimed that there was a small increase in the pressure drop when MFF was used. For the counter-flow mode, a higher convection heat transfer coefficient was observed, and this enhancement increased with increasing Reynolds number
Targui and Kahalerras [4]	numerical	(Pr = 7), a porosity= 0.95, inertia coefficient= 0.35, a Reynolds number Re = 300, a mass flow rate ratio Rm= 1,	The optimal thermal design that found at the utilization of the porous structures on the inner surface of the outer pipe and on the outer surface of the inner pipe. Also, the heat transfer rate was increased when the thickness of the porous structure was increased and therefore the distances were reduced
Kahalerras and Targui [20]	numerical	Pr is set fixed at 7 ($10^{-6} \leq Da \geq 10^{-1}$	The parameters that took in the study are; fin height, fins spacing and the ratio of the thermal conductivity. Their results showed that the rate of heat transfer can enhance compared with the case of fluid, as well as the geometry of the fin and each of the thermodynamic and physical properties, plays important role in the improvement of heat transfer
Chen et al [21]	numerical	porosity of 0.8–0.95 and pore density of 5–30 PPI	The effectiveness of counter flow with foam insert presents 37.5% higher than the parallel flow. whereas the maximum performance factor occurs

			at 15 PPI for different porosities
Rashidian and Tavakoli [12]	numerical	(Re =10,000 to 80,000)	The study concluded that the efficiency of heat exchangers can be improved by using porous materials in the flow path
Moghadasi et al [22]	numerical	Darcy number (10^{-4}–10^{-1})	The average Nusselt number increased by the decrease of Darcy number from 0.1 to 0.0001 and enhancement of the porous thickness ratio.
Benmerkhi et al [23]	numerical	20(PPI) (Re= 200 -1000)	The average Nusselt number whose value is more than 5.88 TIME compared the empty ring. The Nusselt number increases with the increase of the Reynolds number.
Orihuela et al. [10]	numerical	aluminum MF (5PPI, 20PPI) the flow rate (20, 85, 150 LPM)	They found that the foam with 20PPI has better performance than 5PPI when the airflow rate is (20 LPM).
Jamarani et al [24].	numerical	copper porosity of φ =0.9, Re =Reo =20000 and K_S/k_f =342.2 (aluminum/water)	They concluded the best performance is 0.7 obtained for the arrangement in which the porous material is in the center of the inner pipe and on the inner surface of the outer pipe, while the optimum thickness is 0.4 for the arrangement in which the porous material is at the inner and outer surfaces of the inner pipe
Abbas et al. [14]	experimental	Re= 2000 - 11000	The researchers concluded that there was an improvement in the convection heat transfer coefficient up to 260%

			when using fins at the inner pipe compared to the case in which the inner pipe is smooth.
Maid et al [15].	experimental	Reynolds number to hot water (4862.9< Re<14633.8) and constant for cold water (Re=2912.2). hot water mass flow rates between (0.06 6-0.198 kg/s) and (0.1997 kg/s) cold water mass flow rate	The factor of enhancement in the convection heat transfer coefficient is 2.074 and the increase in effectiveness is 26.5% as compared to not using a metal pad is their most important finding
Mishra and Nayak [16].	experimental	A temperature hot water range of 40C° to 55C°. cold constant inlet temperature of 28 C°. Mass Flow Rate (kg/second) 0,.118 - 0.266	They concluded that the effectiveness of the exchanger increases as the distance between the baffles decreases and the cold fluid flow rate increases.
Chikh and Allouache [7].	numerical	Water Pr = 3.01. fluid viscosity (J=1). The porosity = 0.95. Flow velocity of water Ucin = 2.5 m/s at the inlet of the annular gap. Re is over 300	When the porous material has a high effective thermal conductivity, there exists a n optimal porous layer thickness that depends on permeability and for which a significant reduction of total entropy generation rate is obtained. Hence, this passive heat transfer enhancement technique has a great merit for thin porous inserts not exceeding about 40%.
Nasser et al [5].	numerical	Porosity $\geq$ 0.89 pore density= 10PPI, Tin =30 C, and Re_{outer}= 2000,	the heat transfer can be greatly enhanced. Style considerations, however, need to be taken care of to prevent conflicts uneconomical optimization resulting from potential increases in fall in Pressure.

Abbasi et al [25].	numerical	Mass flow rate of (2 kg/s). Number of baffles (6, 8, 10), baffle 15 angle (45◦, 90◦, 135◦) and baffle thickness (5, 10, 15, 20 mm). Porosity, "0.5. Permeability, K (m^2) 10^{11}	- Q ⇑ and ΔP ⇑ when N of baffle⇑. - Q ⇑ and ΔP ⇑ when baffle thickness⇑. - Q ⇑ 139% with ΔP ⇑ of 247% compared to smooth one. - ΔP ⇓ 61.3% while Q ⇑ 11.15% compared to solid baffles.
Odabaee and Hooman [26].	numerical	stream velocities, 2.8 and 5.6 m/s	The contrast this means that heat exchangers with metal foam have 2 to 6 times higher factor in efficiency relative to traditional design.
Nawaz et al [17].	experimental	open-cell aluminum metal Foam. Face velocities (0.3 to 7 m/s). Porosity 5,10,20,40 PPI. Coolant flow rate 0,82 (Kg/sec)	They found that there is more than one factor that affects the amount of pressure drop and heat transfer rate in metal foams, also, the hydrothermal performance with metal foams is better than that with louver-fin
Ibrahim et al [27]	numerical		Their study concluded that the use of fins is beneficial for the thermal performance of latent heat storage systems.
Zhao et al [30]	numerical and experimental	Re= (5000 – 50000). ε =0.9 ϕ=20ppi	The results obtained show that the porous fins heat exchanger improves by 77% and the pressure decreases by 18.5% and the weight of the heat exchanger is also reduced. Finned porous by 90% the performance factor that measures temperature and pressure drop has been increased by 41%.

Xu et al [28].	numerical	the porosity less than 0.9 and the pore density greater than 10pp	They came to the conclusion that the porosity and pore density should be less than 0.9 and greater than 10 PPI, respectively, to achieve effectiveness greater than 0.8.
Arasteh et al[29].	numerical	Porosity=0.95	They proved in their studies that optimally distributed and partitioned metal foams enhance heat transfer more economically and that metal foams (low permeability) have higher PEC. Also the introduction of metal foams in the same longitudinal locations in both pipes leads to a higher heat transfer. The average Nusselt number of the porous Inserted region is about ten times of that of the region with no porous medium
Zhao et al[31].	numerical	10 ppi copper-foam porosity = 0.7-0.95. 10 ppi -60ppi	With the rise in pore density (PPI) and the decrease in in porosity. The effectiveness of the exchanger increases the thermal performance is a function of the cross-section ratio of the flux and the pore density of the mineral foam.

Govindani [2]	experimental	(Re= 3000-15000) flow rate = (4, 6, 8, 10, and 12 LPM)	The study concluded that when a rotor assembly strand is used, there is an increase in turbulence in the flow of the fluid, which led to an increase in the rate of heat transfer even more from a normal tub
Thejaraju et al [1].	experimental	Reynolds number 6000 to 30000	the highest value of the Nusselt number was obtained at the Reynolds number = 30000 and the lowest value of the Nusselt number at Reynolds = 6000 with an increase in the performance value when increasing the Reynolds number, and the coefficient of friction decreased by increasing the Reynolds number in each case. Therefore, the value of performance increases with the increase in Reynolds number.
Sertkaya et al [18]	experimental	Reynolds used is ($5x10^3 – 9\ x10^4$)	They concluded that the heat transfer rate of the finned pipe exchangers is greater than that whose pipes are covered with aluminum foam.

Pavel and Mohamad [32]	experimental and numerical	(Re= 1000–4500) ε = 98%	They found that the heat transfer rates are higher by using the porous materials at a reasonable expense of pressure drop as well. Therefore, heat transfer simulation must be performed when using porous metal foams and thermal conductivity.
Sheikholeslami et al [19]	Experimental	Re=(6000 – 12000)	The Nusselt number increases with the number of Reynolds and the number of holes, the friction factor increases with the number of Reynolds and decreases with the number of holes.
Chen et al [33]	Numerical	Re=(1000 – 9000) Cold water flow rate (m3/s) $3.14x10^{-5}$- $1.57x10^{-4}$	The performance parameter of the double pipe heat exchanger with metal foam remains higher than that of the ordinary double pipe heat exchanger.
Alkam and Al-Nimr [34].	experimental and numerical		They concluded in their study that using an appropriate thickness of the substrates leads to further improvement in the performance of the heat exchanger.

Targui, and Kahalerras [35]	Numerical	water, a porosity= 0.95, an inertia coefficient= 0.35, a Reynolds number Re = 300, a mass flow rate ratio Rm= 1	Their study concluded that the use of the simultaneous flow of porous barriers and a pulsating flow enhances the heat transfer and increases thermal-hydraulic of the heat exchanger.
Present work	Experimental	Water, porosity = 0.95, PPI=15, 2800<Re<32000, constant internal hot air, variable cold air in the annular gap.	Different arrangement of the MF showed that lower amount of the MF could provide higher Nu according to its configuration, and high PEC obtained at low Re.

2.5 Summary of Literature Review

1. The majority of researchers in this field concluded that the use of porous medium leads to an increase in heat transfer and thus to an increase in the thermal performance as well as a relative increase in the pressure drop. All these parameters differ from one research to another according to the design of the device and the quality and dimensions of the foam. Researchers also agreed that the counter flow in the double pipe heat exchanger leads to an improvement in performance greater than the parallel flow.
2. investigated the effect of fully and partially filled annulus using the current proposed configurations and arrangements, which will be described later on the heat transfer and PEC.

CHAPTER THREE
EXPERIMENTAL SETUP AND METHODOLOGY

3.1 Introduction

The flowchart, explained in Fig.(3.1), briefly illustrates the most prominent stages of the experimental work. The first step of the experimental work included the design and fabrication of the rig system. Then all parts have been fixed and a calibration has been carried out to the thermocouples. After doing uncertainty analysis, the tests were run the data were collected after reaching the steady state. The main parameters were calculated from the data which were collected. These parameters were depicted and analyzed. All results obtained for each of the cases studied are analyzed, a comparison is made between them to get the best case among the other cases.

The experiment setup consists of concentric double pipe test section air blowers, heating system, flow meters, manometers, thermometer, and power supply system, as shown schematically in Fig.(3.2) and photographically in Fig.(3.3). Each part is explained in detail in the following sections.

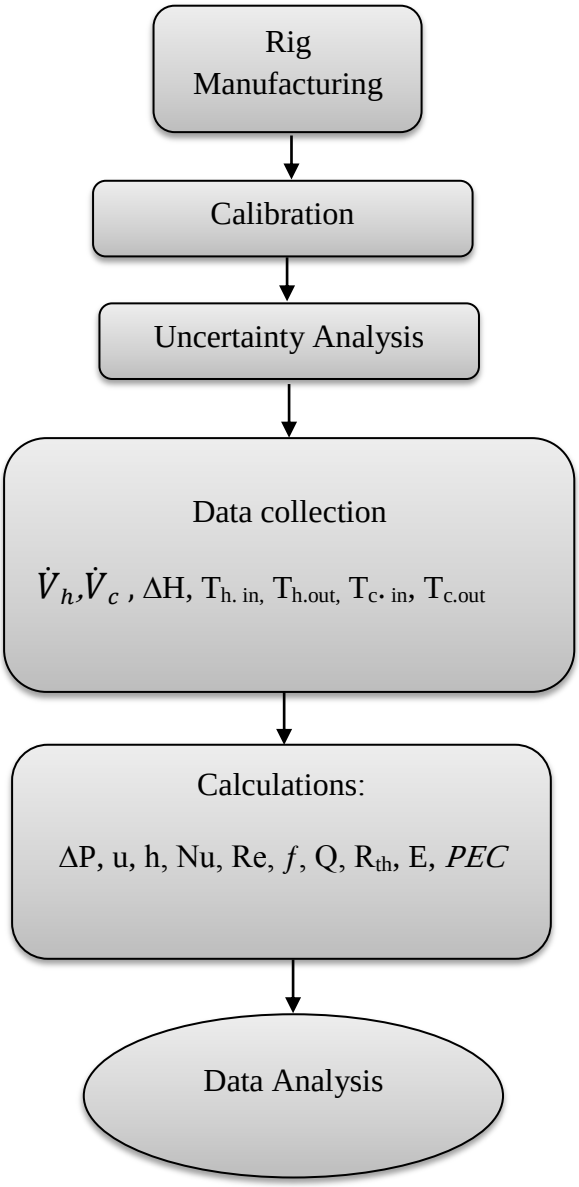

Figure 2.1 Flowchart of the current study.

3.2 Experimental Setup

3.2.1 Test Section

The test section consists of two concentric pipes. The copper pipe is fixed inside the PVC pipe using. PVC connectors and rubber chips and prevent cold air from leaking out of the test section. The test section is fixed on the steel structure by screws. The inner pipe is made of copper, 500 mm long, 17 mm inner diameter, and 19 mm outer diameter. The upstream end of the hot side is connected to the heating system by a galvanized pipe, while the downstream end is open to the surrounding for discharging the hot air. The external PVC pipe has an inner diameter of 42 mm and insulated from the outer surface by Rubber insulation. The hot air passes through the inner pipe while the cold air flows through the gap between the two pipes. Where the heat transfer occurs between the two fluids at different temperatures without contact between them .The notation of the inner and outer diameters of both cylinders are show in Fig. (3.4).

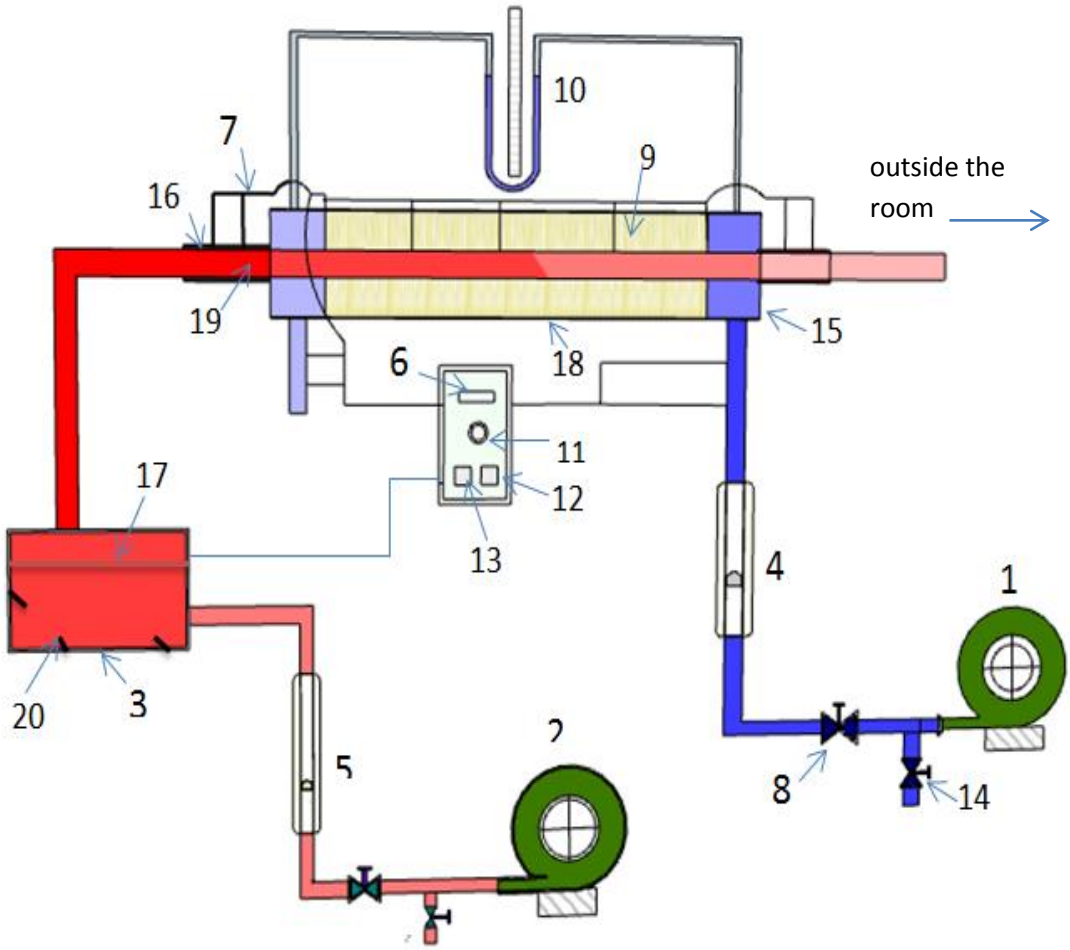

1	Cold air blower	11	Selector switch
2	Hot air blower	12	Power supply
3	Air heating system	13	voltmeter and ammeter
4	Cold Air flow meter	14	Bypass
5	Hot Air flow meter	15	Test section
6	Digital display	16	Insulator
7	Thermocouples	17	Heater 1000 W
8	Gate valve	18	Outer pipe (PVC)
9	Metal foam	19	Inner pipe (copper)
10	U-Tube manometer	20	Fins

Figure 2.2 Schematic of experimental apparatus.

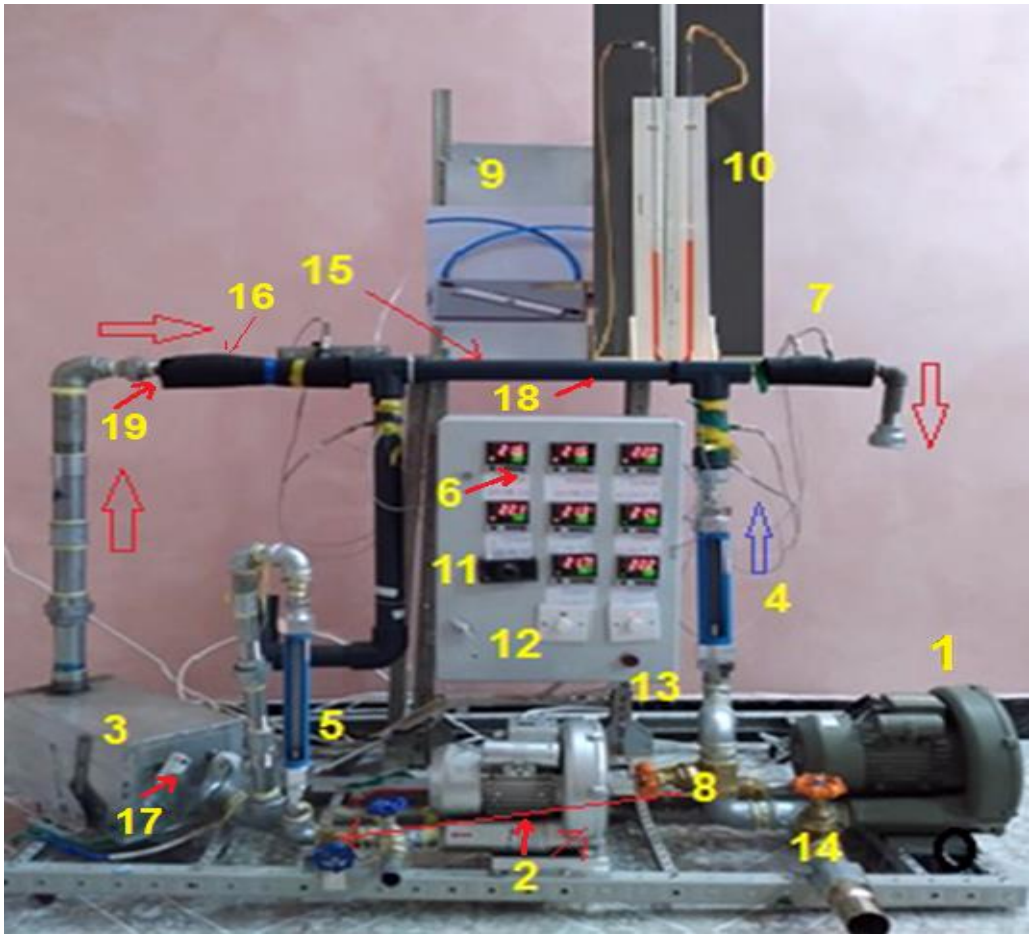

1	Cold air blower	11	Selector switch
2	Hot air blower	12	Power supply
3	Air heating system	13	voltmeter and ammeter
4	Cold Air flow meter	14	Bypass
5	Hot Air flow meter	15	Test section
6	Digital display	16	insulator
7	Thermocouples	17	Heater 1000 W
8	Gate valve	18	Outer pipe(PVC)
9	Inclined manometer	19	Inner pipe(Copper)
10	U-Tube manometer		

Figure 2.3 Photograph of experimental apparatus.

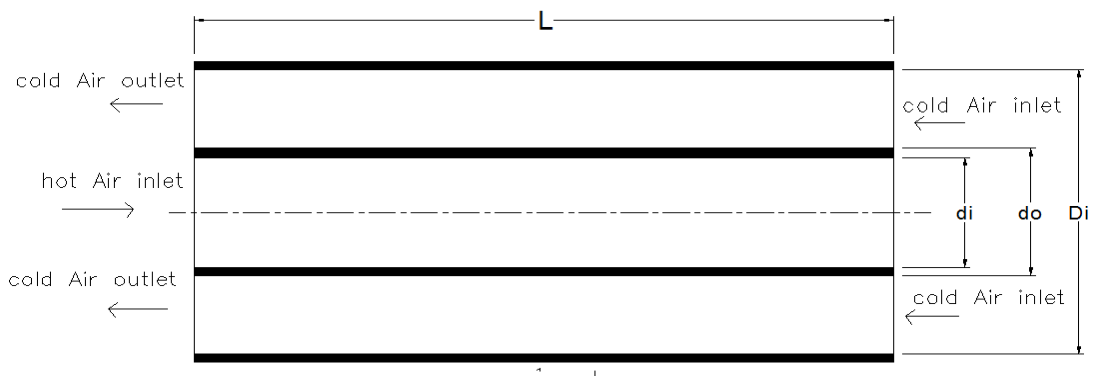

Figure 2.4 Scheme of cross-sectional view of annuls test section.

3.2.2 Metal Foam Arrangement

The sheet of copper metal foam used in this study is of 10 mm in thickness with dimensions (500 × 500 mm^2), (15 PPI), and porosity of (0.95) as shown in Fig. (3.6.a). It is cut by water-jet cutting machine to pieces like washers according to the dimensions required in this study. Fig. (3.6.b) shows the photograph of the washers of metal foam and the mechanism of fixing them in the annular channel. The inner diameter of the washers is identical to the outer diameter of the copper pipe, and the outer diameter of the washers identical to the inner diameter of PVC pipe, as shown in Fig. (3.7.c). The graduation of the MF diameter ratio is shown in Fig. (2.6.d) as from left to right, the (D_{MF}/D_{pipe}) =1.0, 0.75, 0.5, and 0.25, respectively. For full filling the axial length of the annuls, fifty washers of MF are used taking a special care to be in contact, as shown in Fig. (3.6.e). The terminals of the PVC pipe are connected with intake and discharging sections as shown in Fig. (3.6.f).

The copper metal foam is cut into concentric washers with a thickness of 10 mm and at different diameters and fixed through the gap between two pipes. The metal foam washers are fixed in such a way to obtain the required arrangements as shown in Fig. (3.5). The inner diameter of MF washers is 19 mm, while the outer diameter is varied to be (D_{MF}/D_{pipe}) = 0.25, 0.50, 0.75, and 1.0. The details of the cases studied here are described as follows.

1) **Case 1**: the metal foam is formed to fill the whole gap of the annulus along the axial length of the test section. It can be said that the annular gap is filled 100% by the metal foam as shown in Fig. (3.5.a).
2) **Case 2**: the metal foam fills the second-half of the test section completely (D_{MF}/D_{pipe}) = 100% as shown in Fig. (3.5.b).

3) **Case 3**: the metal foam fills the whole axial length of the test section while only 75% of the radial direction is filled by the metal foam (D_{MF} /D_{pipe}) = 75% as shown in Fig. (3.5.c).
4) **Case 4**: the MF washers fill 50% of the annular gap of test section whereas the washer thickness is 10 mm and there is a gap between every two successive washers 10 mm to form a periodic configuration for the metal foam. Thus, only 50% of the annular space is filled with MF as shown in Fig. (3.5.d).
5) **Case 5**: The metal foam is fixed a repeated in pattern with the axial direction along the test section. Each pattern included four metal foam washers. The washers have been arranged to be (D_{MF}/D_{pipe}) = 1.0, 0.75, 0.5, and 0.25, respectively, as shown in Fig. (3.5.e).
6) **Case 6**: The first quarter of the axial length of the test section is filled with metal foam washers that have a (D_{MF}/D_{pipe}) = 0.25. The second, third, and fourth quarter of the axial length have a diameter ratio of 0.5, 0.75, and 1.0, respectively, as shown in Fig. (3.5.f).
7) **Case 7**: The metal foam is fixed a repeated in pattern with the axial direction along the test section. Each pattern included seven metal foam washers. The washers have been arranged to be (D_{MF}/D_{pipe}) = 0.25,0.5,0.75,1.0, 0.75, 0.5, and 0.25, respectively, as shown in Fig. (3.5.g).
8) **Case 8**: This case is tested without metal foam (smooth) and the gap between the two pipes is completely empty as shown in Fig. (3.5.h).

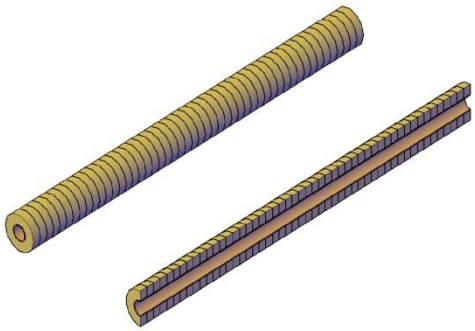

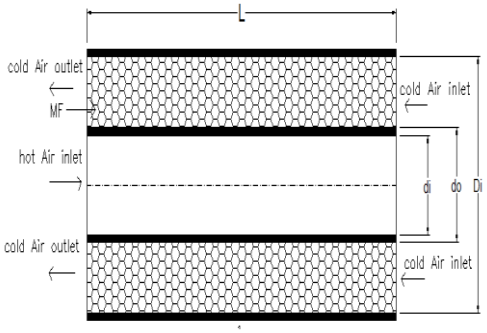
L
cold Air outlet
MF
hot Air inlet
cold Air outlet
cold Air inlet
di
do
Di
cold Air inlet

(a)

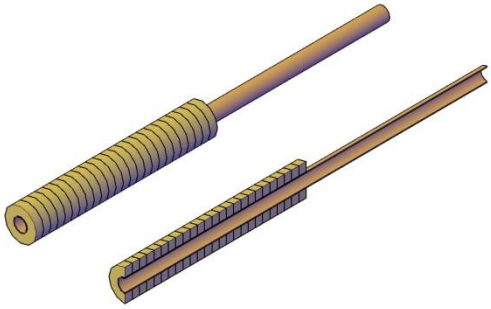

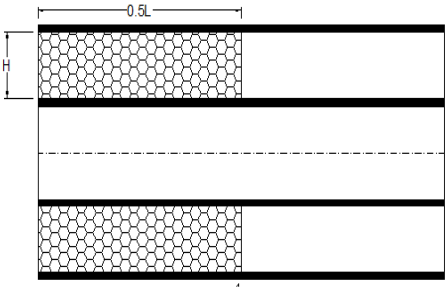
0.5L
H

(b)

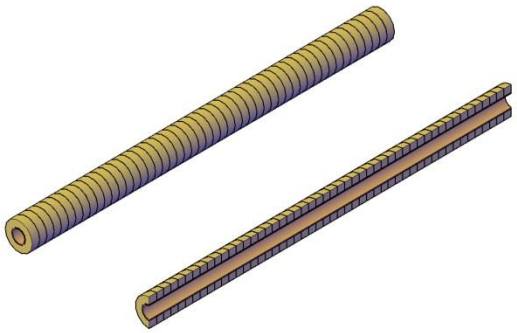

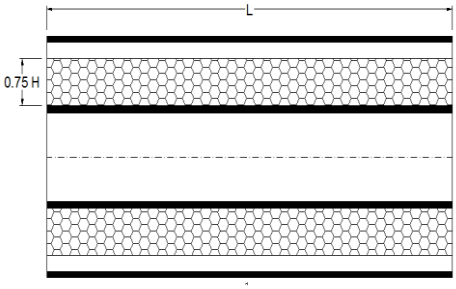
L
0.75 H

(c)

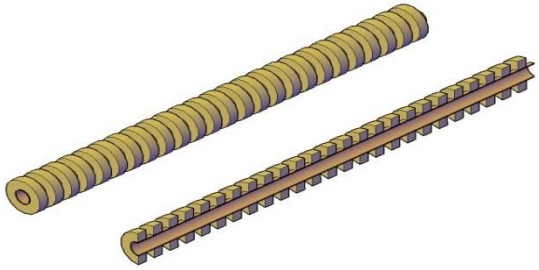

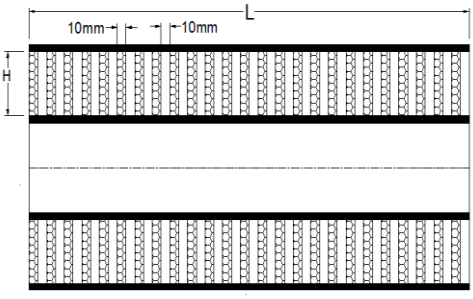
L
10mm
10mm
H

(d)

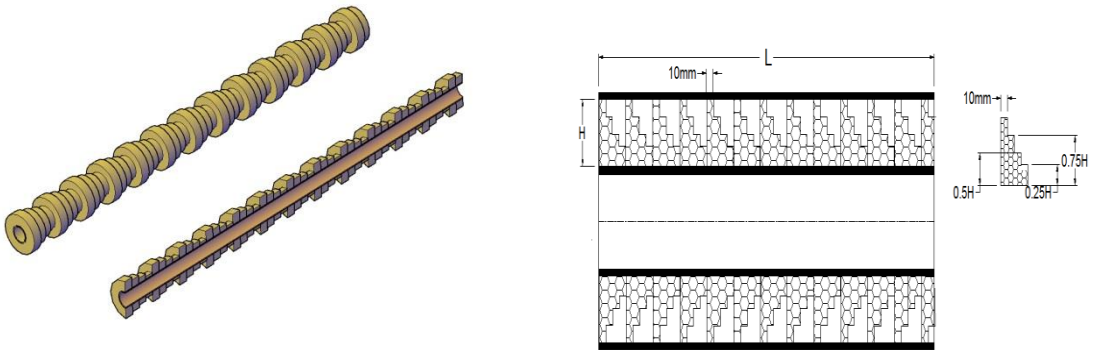

(e)

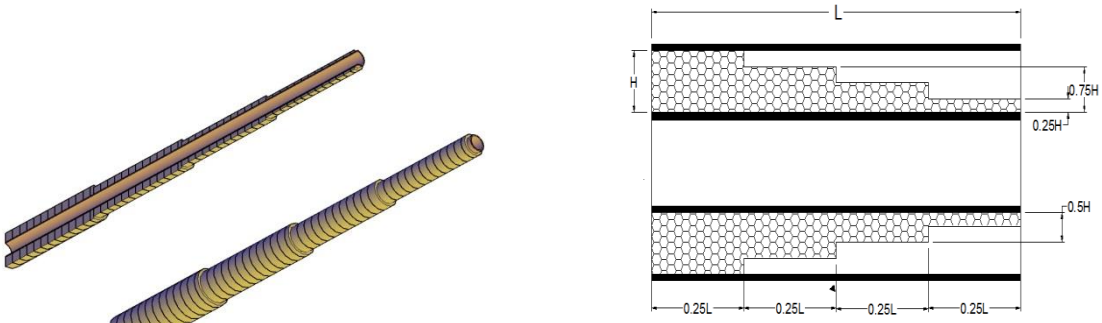

(f)

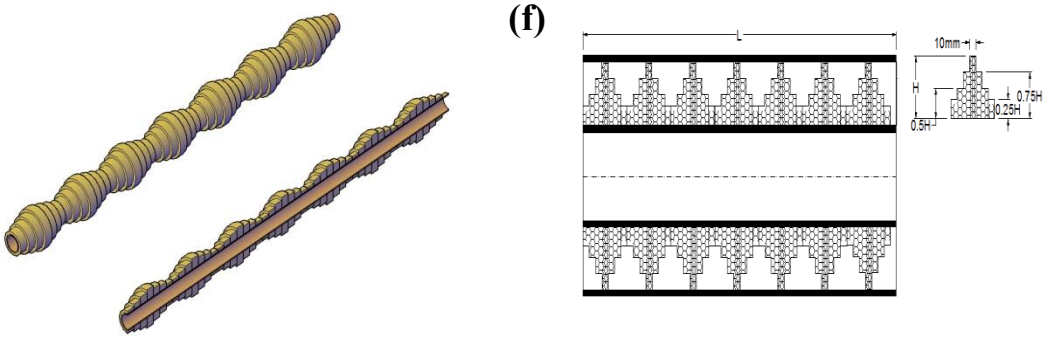

(g)

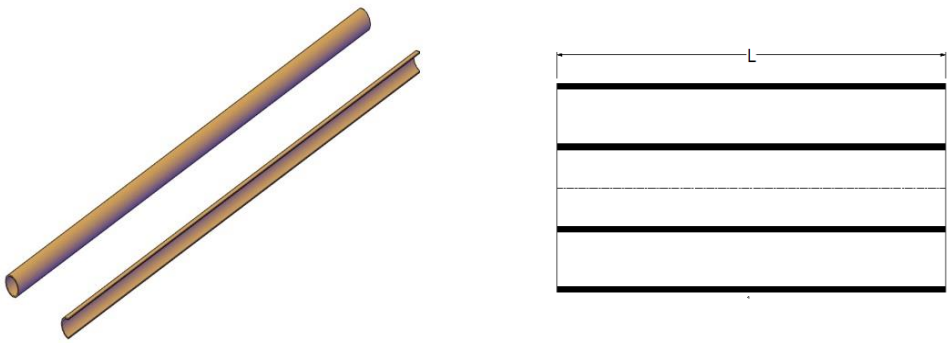

(h)

Figure 2.5 Distribution of metal foam along the copper pipe.(a) case 1, (b) case 2, (c) case 3, (d) case 4, (e) case 5, (f) case 6,(g) case 7,(h) case8

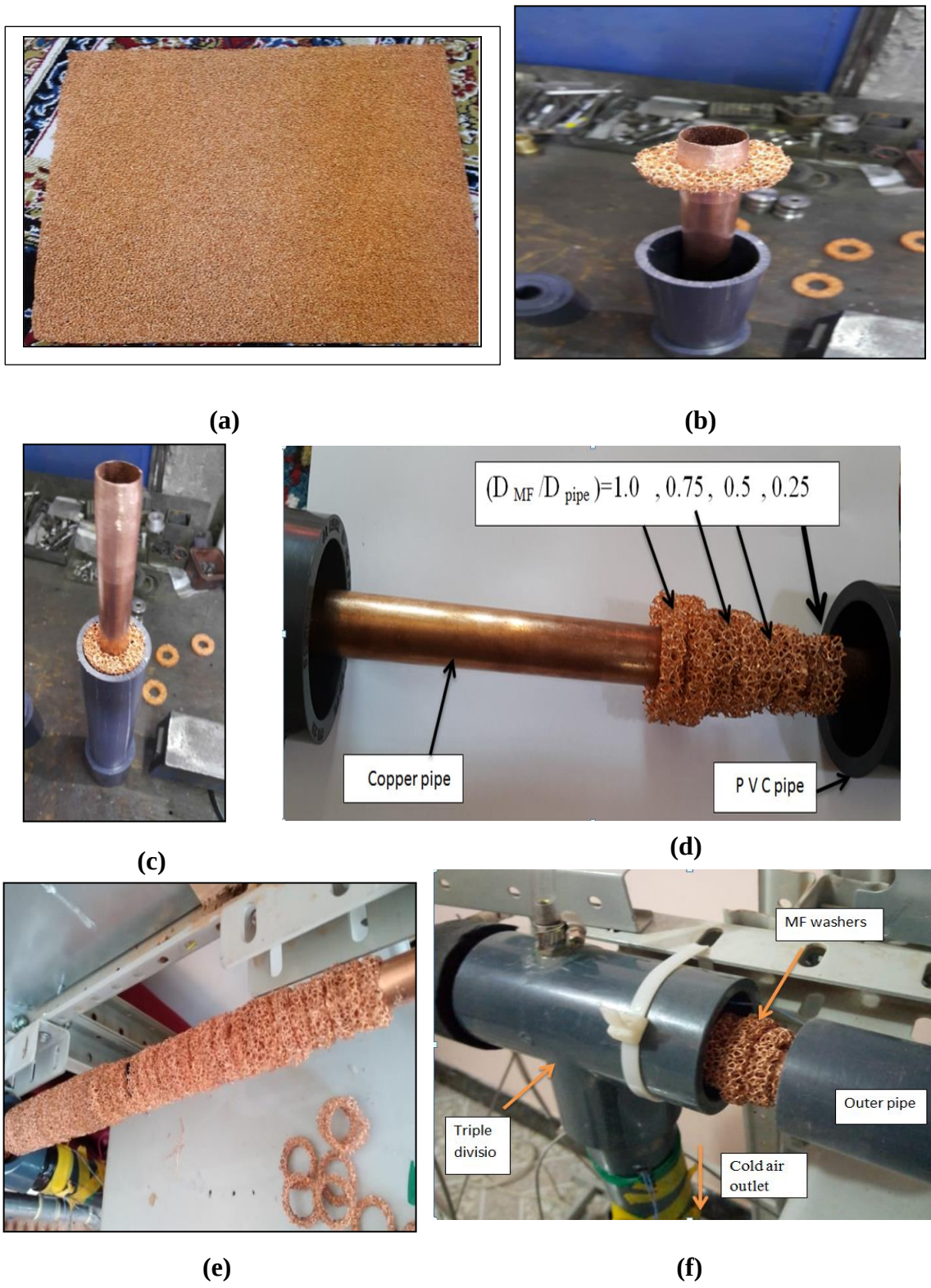

Figure 2.6 Photo of metal foam; (a) copper MF plate, (b) MF washer, (c) MF insertion,(d) MF configuration, (e) MF arrangement (case1), (f) test section fixing with MF

3.3 Air Blowers

The cold air blower of (OFFICINE AUGUSTO CATTANI, ITALY) with power consumption of (750W), maximum flow (124 m^3/h), and maximum pressure (–130/140 mbar) with a speed of 2800 rpm is used for forcing air to the cold air side. It is used to blow the cold air within the gap between the two pipes as shown in Fig. (3.7.a). The amount of cold air is controlled using two manual control valves, one is for adjusting the air flow rate passing through the test section, whereas another is used for discharging the redundant air outside the system via the bypass. The hot air blower of (OFFICINE AUGUSTO CATTANI, ITALY) with a power consumption of (370W), maximum flow (80 m^3/h), and maximum pressure (–130/120 mbar) employed to force the hot air inside the copper pipe as shown in Fig. (3.7.b). The flow rate of the hot air can be controlled accurately by using a valve of bypass. Several flow rates of cold air are covered throughout this study, while the flow rate of the hot air is kept constant.

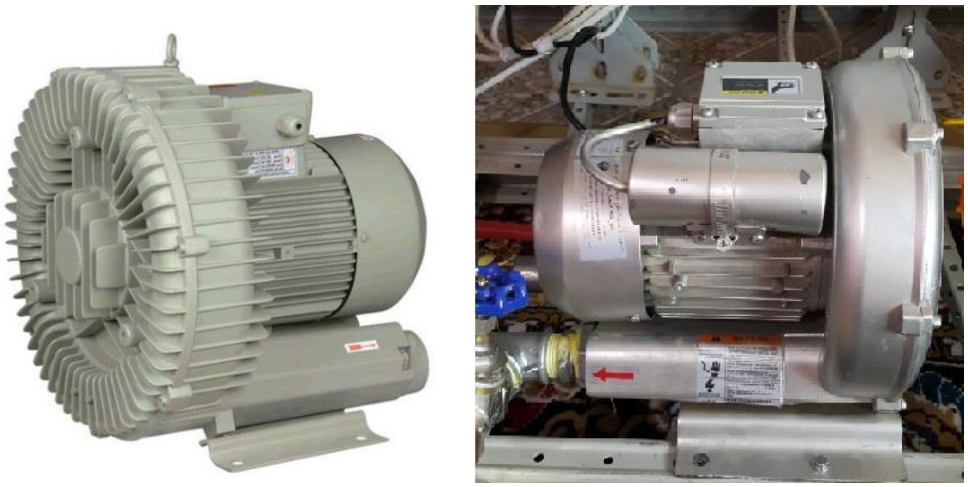

(a) (b)

Figure 2.7 Air blowers; (a) cold air blower and (b) hot air blower.

3.4 The Heating System

An electrical heating system is used for heating the air of the hot stream as shown in Fig. (3.8). The heating system is made of steel box, with dimensions of (400 × 200 × 200) mm^3 sealed completely. For getting good air mixing inside the heating system box, the inlet and exit holes (with a diameter of 37.5 mm) designed to be in a normal direction and several vortex generators are fixed inside the box. Two electrical heaters with a capacity of (1000 W) for each are used. The temperature of inlet hot air is controlled by adjusting the heater power.

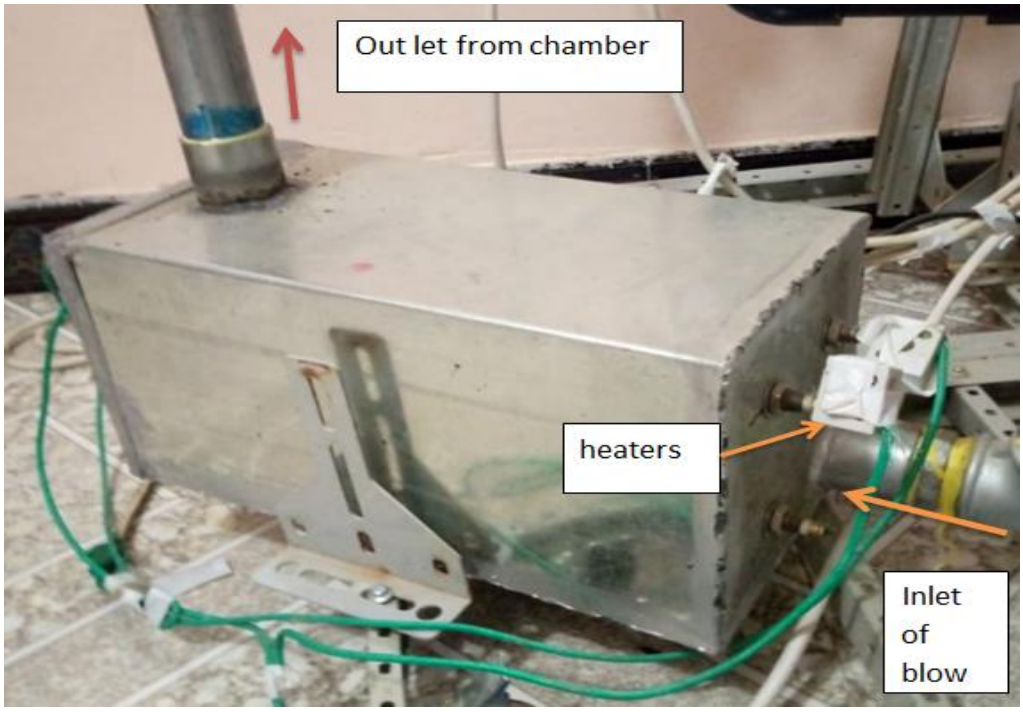

Figure 2.8 Heating system.

3.5 Data acquisition system

3.5.1 Pressure Measurement

The pressure drop along the cold air side of the annulus is measured using an inclined manometer for smooth heat exchanger due to small pressure drop as shown in Fig. (3.9.a). The specific gravity of the fluid of the inclined manometer is 0.75. It is connected to two taps, one at the upstream end and another at the downstream end of the annulus. The holes of the taps are drilled and smoothened from the internal surface of the outer pipe to avoid the flow separation due to the metal chips. In the case of using metal foam, the pressure drop is high, and therefore, a U-tube manometer is used to satisfy the maximum pressure predicted through it, as shown in Fig. (3.9.b).

(a) **(b)**

Figure 2.9 Pressure drop devices; (a) inclined manometer, (b) U - tube manometer.

3.5.2 Temperature Measurement

The air temperatures of the two fluids and the cylinder surface in the heat exchanger are measured by using thirteen thermocouples type-K (accuracy ±1%). Two thermocouples are fixed at each of the inlet and outlet of the cold and hot streams to measure the average air bulk temperature. The probes of thermocouples are fixed at the mid-distance of the flow pipe. In order to measure the surface temperature of the copper pipe of the test section, five thermocouples are installed in a V-grooves created on the outer surface, as shown in Fig. (3.10). The positions of T_{s1}, T_{s2},T_{s3}, T_{s4}, and T_{s5}, are 0, 100, 250, 400, and 500 mm relative to hot air inlet.

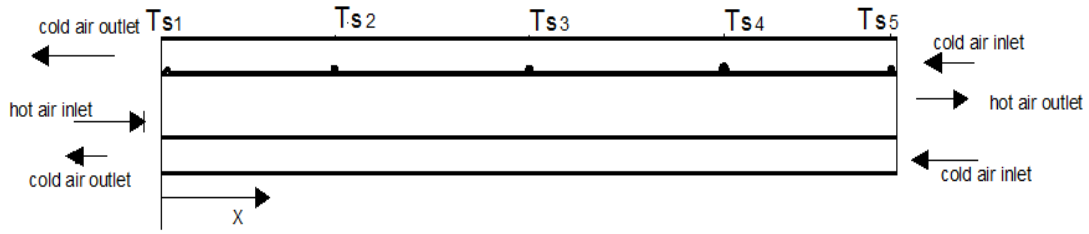

Figure 2.10 Schematic diagram of thermocouples distribution on the outer surface of the copper pipe.

The thermocouples displayed in Fig. (3.11.a) are connected to digital displays, which has one digit after the decimal. The display type is of (Maxwell, MTD-72) (Accuracy: ±0.3 % FS) and (power supply: 85-265 VAC) as shown in Fig. (3.11.b).

A selector switch Model (TEMPCON) is used to connect the thermocouples with the digital display. The selector switch contains (12) channels Fig. (3.11.c) shows a photographing for the selector switch. A regulator of the power supply is used for adjusting the heating power which is shown in Fig. (3.11.d).

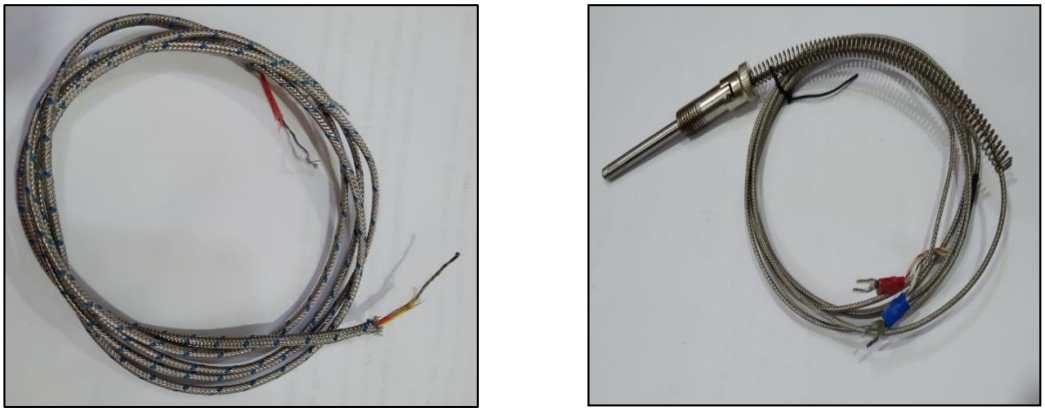

(a)

(b)

(c)

(d)

Figure 2.11 Temperature measuring devices; (a) Thermocouple type-K, (b) Digital Temperature controller, (c) Selector unit, (d) power supply.

3.5.3 Air Flow Rate Measurement

The cold air flow rate is measured by rotary flow meter type (VA1OS-25) with a range of (3-50 m^3/h), (accuracy; ±5%), working temperature (–20 to 120 °C), and working pressure (≤ 1.0 Mpa) as shown in Fig. (3.12.a). It is installed before the test section. Whereas, the amount of hot air is measured by another rotary flow meter (VA10S-15) with a range of (1.2 – 12 m^3/h), (accuracy; ±5%), working temperature (–20 to 120 °C), and working pressure (≤1.0 Mpa) as shown in Fig. (3.12.b), which is fixed before the heating system. The amount of the cold and hot air is controlled manually by the valves and the bypass is used for getting the small amounts of flow rats.

(c)

(d)

Figure 2.12 Air flow meters; (a) Type (VA1OS-25), (b) Type (VA10S-15).

3.6 Methodology

3.6.1 Data Reduction

After collecting the data from the experimental measurement, the main parameters essentially required for evaluating the performance of the proposed design of the double pipe heat exchanger are calculated as shown below. The main parameters are the Reynolds number, heat transfer coefficient, local and average Nusselt number, friction factor, Effectiveness, and performance evaluation criteria. The mass flow rate of air is estimated from [14]

$$\dot{m} = \dot{V} \times \rho_{air} \tag{3.1}$$

where $\dot{m}$ is the mass flow rate (kg/s), $\dot{V}$: is the volumetric flow rate of air (m^3/s), and ρ: indicates the density of air (kg/m^3).

The hydraulic diameter $(D_{h\,o})$ of the annular section is estimated by:

$$D_{ho} = \frac{4A_c}{p} = \frac{4\times(\frac{\pi}{4})({D_i}^2 - {d_o}^2)}{\pi D_i + \pi d_o} = D_i - d_o \tag{3.2}$$

where p: the wetted perimeter (m). while for the inner pipe, the hydraulic diameter is the cylinder diameter $D_{h\,i} = d_i$.The velocity and Reynolds number was estimated using the following equation [14]:

$$u = \frac{\dot{V}}{A_c} = \frac{4\dot{V}}{\pi(D_h)^2} \tag{3.3}$$

$$\mathrm{Re} = \frac{\mathrm{D_h u\,\rho}}{\mu} = \frac{\mathrm{D_h}\,\frac{4\dot{V}}{\pi {\mathrm{D_h}}^2}}{\frac{\mu}{\rho}} = \frac{\mathrm{D_h}\,\frac{4\frac{\dot{m}}{\rho}}{\pi {\mathrm{D_h}}^2}}{\frac{\mu}{\rho}}$$

$$Re = \frac{4\dot{m}}{\pi D_h\,\mu} \tag{3.4}$$

μ : viscosity of air N. s / m^2

The heat transfer rate calculations from the hot air to the cold air is calculated according to the following procedure:

- Heat transfer from the hot air is given by [14]:

$$Q_h = \left(\dot{m}C_p\right)_h \left(T_{h,i} - T_{h,o}\right) \tag{3.5}$$

- Heat transfer to cold air is given by [14] :

$$Q_c = \left(\dot{m}C_p\right)_c \left(T_{c,0} - T_{c,i}\right) \tag{3.6}$$

The average heat transfer rate ($\mathrm{Q_{ave}}$) between the hot air and cold air side is [11]:

$$\mathrm{Q_{ave}} = \frac{\mathrm{Q_c + Q_h}}{2} \tag{3.7}$$

The convection heat transfer coefficient (h_i) between the hot air and internal surface of the copper pipe:

$$h_i = \frac{Q_{ave}}{A_i\left(T_{h\ ave} - T_{\mathrm{s\ ave}}\right)} \tag{3.8}$$

To calculate the average temperature of cold air ($T_{c,ave}$), the average temperature of hot air ($T_{h,ave}$), and average wall temperature, respectively;

$$T_{h,ave} = \frac{(T_{hi} + T_{ho})}{2} \tag{3.9}$$

$$T_{c,ave} = \frac{(T_{ci} + T_{co})}{2} \tag{3.10}$$

$$T_{\mathrm{s_{ave}}} = \frac{\mathrm{T_{s_1} + T_{s_2} + T_{s_3} + T_{s_4} + T_{s_5}}}{5} \tag{3.11}$$

$T_{s_{ave}}$: the average temperature of outer surface of copper pipe.

The log mean temperature difference ΔT_{LM}, as shown in Fig. 3.13, for counter flow double - pipe heat exchanger is estimated from the following equation [28].

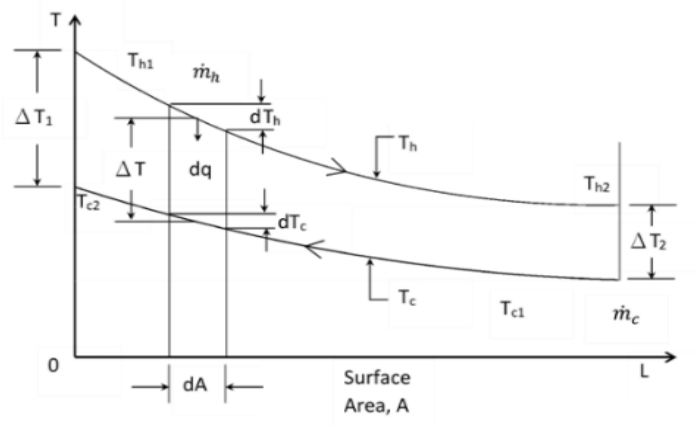

(a)

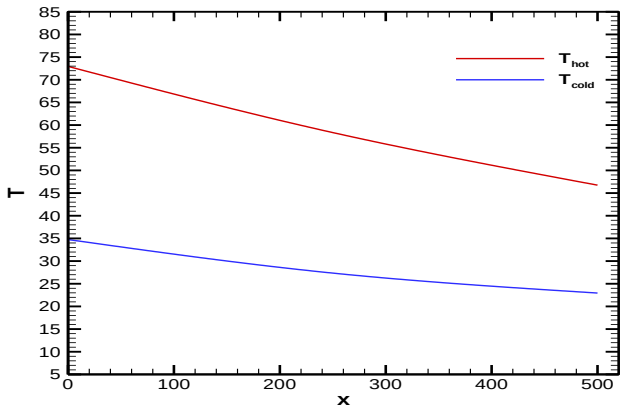

(b)

Figure 2.13 Fluids Temperature variation of counter flow double pipe heat exchanger . a.[14], b. current experimental.

$$\Delta T_{LM} = \frac{(T_{hi} - T_{co}) - (T_{ho} - T_{ci})}{ln[((T_{hi} - T_{co})/(T_{ho} - T_{ci})]} \quad (3.12)$$

The overall heat transfer coefficient U_i is calculated as follows [11]:

$$U_i = \frac{Q_{ave}}{A_i \Delta T_{LM}} \quad (3.13)$$

The convection heat transfer coefficient of cold air (h_o) is calculated from the overall thermal resistance [27]

$$h_o = \frac{1}{A_o\left(\frac{1}{UiAi} - \frac{1}{hiAi} - \frac{\ln\left(\frac{d_o}{d_i}\right)}{2\pi kL}\right)} \quad (3.14)$$

where: $A_o = \pi\, L\, d_o$

The average Nussle number (Nu_{av}) on the outer surface of the inner cylinder can be expressed as follows:

$$Nu = \frac{h_0\, D_{h\,o}}{k} \quad (3.15)$$

The effectiveness of the double-pipe heat exchanger (E) is estimated from [13]:

$$E = \frac{Q_{ave}}{Q_{max}} \quad (3.16)$$

The maximum heat transfer can be given as[13]:

$$Q_{max} = \left(\dot{m}C_p\right)_h\left(T_{h,i} - T_{c,i}\right) \quad (3.17)$$

The pressure drop in the annular side is calculated by:

$$\Delta P = \rho \times g \times \Delta H \quad (3.18)$$

The friction factor (f) is calculated for the cold stream using the following equation [11]:

$$f = \frac{\Delta P\left(\frac{D_h}{L}\right)}{\rho u^2/2} \quad (3.19)$$

The performance evaluated criteria of the double-pipe heat exchanger (PEC) for cold air side [11]:

$$PEC = \frac{(\frac{Nu_{MF}}{Nu_s})}{(\frac{f_{MF}}{f_s})^{\frac{1}{3}}} \quad (3.20)$$

It is worth mentioning that the hot and cold air properties were estimated by using the following correlations which were correlated from the data of air properties [6], for a wide range of temperature (0–100 °C).

The data was correlated by using curve expert software for determining $k, C_p, \mu, and\ \rho$ as function of temperature for hot and cold air:

$$\mathrm{k} = 2.36 \times 10^{-2} + 7.59 \times 10^{-5} \times \mathrm{T_{ave}} - 3.39 \times 10^{-8} \times \mathrm{T_{ave}^2} + 1.33 \times 10^{-10} \times \mathrm{T_{ave}^3} - 6.16 \times 10^{-13} \times \mathrm{T_{ave}^4} \quad (3.21)$$

$$C_p = 1.01 \times 10^3 + 1.49 \times 10^{-1} \times T_{ave} - 4.19 \times 10^{-3} \times T_{ave}^2 + 4.52 \times 10^{-5} \times T_{ave}^3 - 1.44 \times 10^{-7} \times T_{ave}^4 \quad (3.22)$$

$$\mu = 1.73 \times 10^{-5} + 4.75 \times 10^{-8} \times T_{ave} + 4.58 \times 10^{-11} \times T_{ave}^2 - 2.96 \times 10^{-12} \times T_{ave}^3 + 5.00 \times 10^{-13} \times T_{ave}^4 - 3.84 \times 10^{-16} \times T_{ave}^5 + 1.09 \times 10^{-18} \times T_{ave}^6 \quad (3.23)$$

$$\rho = 1.2918369 - 4.69 \times 10^{-3} \times T_{ave} + 1.53 \times 10^{-5} \times T_{ave}^2 - 3.03 \times 10^{-8} \times T_{ave}^3 + 4.99 \times 10^{-12} \times T_{ave}^4 \quad (3.24)$$

3.7 Range of Variables

The parameters and their values/ranges adopted in the current study are included in Table 3.1. Some parameters were kept constant such as: porosity, and pores per inch, while the others were variable along the study where ΔT, $\dot{m}$, and Re,

Table 2-1 Variable range

No	Variable	Range/value
1	Reynolds number (Re) cold air	≈ 2770 – 32,880
2	Reynolds number (Re) hot air	≈ 2765 constant
3	Air temperature difference (ΔT) $\Delta T = T_{h,in} - T_{c,in}$	(20 , 30, 40, and 50 C°)
4	Cold air volumetric flow rate $\dot{V}_c$	(0.0008 – 0.01 m^3/s)
5	Hot air volumetric flow rate $\dot{V}_h$	0.0008 m^3/s
6	Pores per inch	15 PPI
7	Porosity (ε)	0.95
8	Air Ratio	1,2,4,6

3.8 Experimental Procedure

The following steps represent the procedure of the experiments.

1. The two blowers were turned on first. The power supply of the heaters in the heating system was switched on and the voltage and current were adjusted according to the required air bulk temperature at the inlet of hot side.
2. The air flow rate of the hot and cold side were controlled by adjusting the valves of the blowers. The cold air flow rate was

varied according to the requirement of the test, while the hot air flow rate was kept constant.

3. The system was left to work until the cold and hot air temperatures become steady state.
4. The temperature of the hot and cold air at the inlet and outlet, copper surface temperatures, pressure head, and the flow rates of both cold and hot air were recorded.
5. Changing the cold air flow rate (i.e., Re) and repeating steps (1– 4).
6. Changing the metal foam configuration and repeating the steps (1-5).
7. The temperature difference (ΔT) was also changed each time (20, 30, 40, and 50 °C), for three cases only ; 1,2, and 8

3.9 Sample of Calculation

A sample of calculations is made for case 1 where the value of ΔT was fixed at $50°C$. The given data are:

$\dot{V}_C$=3 m^3/h =0.0008 m^3/s

$\dot{V}_h$ =3 m^3/h =0.0008 m^3/s

$T_{hi} = 70.75\ °C$

$T_{ho} = 44.25°C$

$T_{ci} = 20.75\ °C$

$T_{co} = 32.15\ °C$

$T_{h\,ave} = \frac{(70.75+44.25)}{2} = 57.5°C$

$T_{c\,ave} = \frac{(20.75+32.15)}{2} = 26.45\ °C$

The air properties were estimated of film temperatures, and they are reported in table 3.2

Table 2-2 The other variables are calculated as follow:

Air properties	Hot air	Cold air	unite
k	--------	0.02562	$W/m.℃$
C_p	1006.98	1007.03	$J/kg.℃$
μ	1.997×10^{-5}	1.856×10^{-5}	$N.S/m^2$
ρ	1.067	1.1780	kg/m^3

$$AR = \frac{\dot{V}_C}{\dot{V}_h} = \frac{3}{3} = 1 \qquad (3.25)$$

$$\Delta T_{LM} = \frac{(70.75-32.15)-(44.25-20.75)}{ln[((70.75-32.15)/(44.25-20.75)]} = 30.42\ ℃$$

$$\dot{m}_c = 0.0008 \times 1.1780 = 9.424 \times 10^{-4}\ kg/s$$

$$\dot{m}_h = 0.0008 \times 1.0670 = 8.536 \times 10^{-4}\ kg/s$$

$$Q_h = (8.53 \times 10^{-4} \times 1006.98)_h(70.75 - 44.25) = 22.779\ W$$

$$Q_c = (9.424 \times 10^{-4} \times 1007.03)_c(32.15 - 20.75) = 10.819\ W$$

$$Q_{ave} = \frac{10.819+22.779}{2} = 16.8\ W$$

$$T_{s_{ave}} = \frac{49.25+37.7+35+31.9+31.7}{5} = 37.12\ ℃$$

$$Q_{max} = (8.53 \times 10^{-4} \times 1006.98)_h(70.75 - 20.75) = 42.97\ W$$

$$E = \frac{16.8}{42.97} = 0.39$$

$$A_i = 3.14 \times 0.5 \times 17 \times 10^{-3} = 0.0267\ m^2$$

$$A_o = 3.14 \times 0.5 \times 19 \times 10^{-3} = 0.02983\ m^2$$

$$h_i = \frac{16.8}{0.0267(57.5\ -37.12)} = 30.87\ \mathrm{w/m^2.^{\circ}C}$$

$$U_i = \frac{\mathbf{16.8}}{0.0267 \times \mathbf{30.42}} = 20.68\ \mathrm{w/m^2.^{\circ}C}$$

$$h_o = \frac{1}{0.02983(\frac{1}{20.68 \times 0.0267} - \frac{1}{30.87 \times 0.0267} - \frac{\ln\left(\frac{0.019}{0.017}\right)}{2 \times 3.14 \times 0.02562 \times 0.5})}$$

$$= 56.1\frac{W}{\mathrm{m^2}}.^{\circ}\mathrm{C}$$

$$\mathrm{D_h} = (0.042 - 0.019) = 0.023\mathrm{m}$$

$$Nu = \frac{56.1 \times 0.023}{0.02562} = 50.36$$

$$Re_c = \frac{4 \times 9.424\mathrm{x}10^{-4}}{\pi \times 0.023 \times 1.856 \times 10^{-5}} = 2811$$

$$\Delta P = 1000 \times 9.81 \times 5 \times 10^{-3} = 49.05\ Pa$$

$$\mathrm{u} = \frac{0.0008}{0.000415} = 1.93\ \mathrm{m/s}$$

$$f = \frac{49.05(\frac{0.023}{0.5})}{1.1780 \times 1.93^2/2} = 1.033$$

$$PEC = \frac{(\frac{50.368}{16.34})}{(\frac{1.0332}{0.0625})^{\frac{1}{3}}} = 1.21$$

3.10 Uncertainty Analysis

The uncertainties of the experimental instrument for parameters such as Nusselt number, Reynolds number, and friction factor were calculated in the current study based on the Kline [37]

Given a dependent parameter,

$$R = R(X_1 + X_2 + X_3 + \cdots \ldots + X_n) \qquad (3.26)$$

where, $X_1, X_2, X_3, \ and \ X_n$ are independent measured parameters. Therefore, the uncertainty of R can be calculated as follows:

$$U_R = \pm\sqrt{\left(\frac{\partial R}{\partial X_1}U_{X_1}\right)^2 + \left(\frac{\partial R}{\partial X_2}U_{X_2}\right)^2 + \left(\frac{\partial R}{\partial X_3}U_{X_3}\right)^2 + \cdots + \left(\frac{\partial R}{\partial X_n}U_{X_{n1}}\right)^2} \quad (3.27)$$

where $U_{X_1}, U_{X_2}, U_{X_3}$, and U_{X_n} the uncertainties of independent parameters.

The partial derivatives $\frac{\partial R}{\partial X_1}, \frac{\partial R}{\partial X_1}, \frac{\partial R}{\partial X_1}, \ldots \ldots \frac{\partial R}{\partial X_1}$ estimate from eq. (3.26).

Table 2-3 The accuracy of parameters.

NO	Variables	Accuracy
1	The length of channel, L	±1.0 mm
2	The inner diameter of inner pipe, d_i	±0.1 mm
3	The outer diameter of inner pipe, d_o	±0.1 mm
4	The inner diameter of outer pipe, D_i	±0.1 mm
5	Inlet cold air temperature, $T_{c,in}$	±0.93%
6	Outlet cold air temperature, $T_{c,o}$	±0.93%
7	Inlet hot air temperature, $T_{h,in}$	±0.93%
8	Outlet hot air temperature, $T_{h,o}$	±0.93%
9	Surface temperature, T_s	±0.93%
10	flow rate, m^3/h	±5.0%
11	Pressure head, ΔH	±1mm

CHAPTER FOUR
RESULTS AND DISCUSSION

4.1 Introduction

Due to the development in various industries that use heat exchangers, it was considerable to design heat exchangers with high heat transfer performance and low additional pressure drop. Among the most important of these enhancements, the insertion of metal foam in the heat exchangers plays a vital role due to its efficiency in transferring heat and low additional pressure drop compared to pure metal insertions, in addition to the mechanical properties. In this study, two metal foam sheets of copper (15 PPI), porosity (0.95) with dimensions of (500 × 500 mm) and thickness of 10 mm were cut using supersonic air jet machine due to its precise cutting for the edges of the MF to forming a circular metal foam washers. The cutting was done in different dimensions according to the required configuration and arrangement to be studied here. Seven patterns were formed in which the shape and distribution of metal foam were changed to show their superiority in transferring the heat and how much the pressure drop will be raised.

One of the advantages of metal foam is to allow air to pass through it, and this feature does not cause an increase in the pressure drop; smooth, full-filled, and partially/periodically-filled with MF were investigated.

A wide turbulent range of Reynolds number was covered. The results were represented in terms of temperature, average Nusselt number, local Nusselt number, convection heat transfer coefficient, friction factor, and PEC. Seventy tests were conducted in the current study to the purpose of covering all the suggested parameters that we need in the experimental

part. Then, the data obtained in each test were written in order to be analyzed and to present the relationships on the basis of the parameters that were calculated in the research.

4.2 Verification Of The Experimental Apparatus

First of all, the current study is verified before achieving the tests for Nu number, Fig. (4.1.a), and friction factor, Fig. (4.1.b), comparing with the data published by Thejaraju et al. [1] and Blasius's correlation for friction factor for smooth pipe over a wide range of Reynolds number. The deviation between the current study and the Thejaraju et al [1]. was ±7.4% for Nusselt number. The deviation between the current study and, Blasius's correlation and Thejaraju et al [1]was ±7.6%, ±9.2% for friction factor, respectively.

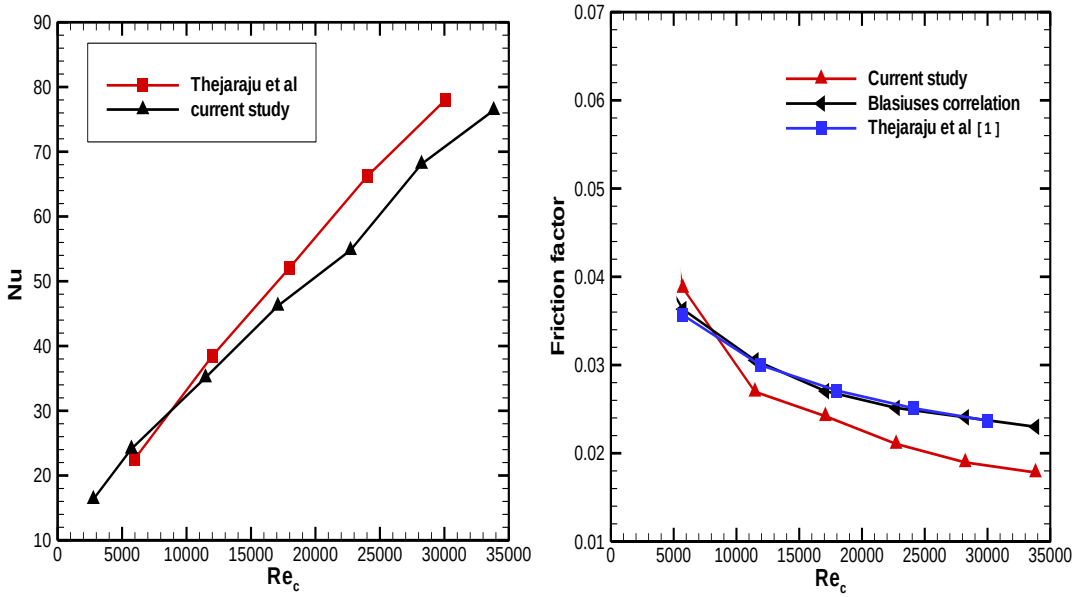

Figure 0.1 Validation of the current experimental setup; (a) Nusselt number with Thejaraju et al [1]. (b) friction factor with the data of Thejaraju et al. and Blasius's correlation, $f = 0.316 \times \mathrm{Re}^{-0.25}$.

4.3 Effect Of ΔT On The Heat Transfer

In this section, the effect of the ($\Delta T = T_{h\ in} - T_{c\ in}$) on the rate of heat transfer represented by Nusselt number is presented in Fig. (4.2) for four values of air ratio. The ΔT_{in} and AR were takes to be (20, 30, 40, and 50 C°) and (1, 2, 4, and 6), respectively. This examination was carried out on the case 8 (empty annulus), case 1 (full filled with MF) as shown in (4.2.a) and Fig. (4.2.b), respectively.

For case 8, the average Nu number is strongly affected by ΔT in particular at high AR. This trend can be also seen in case 1 where the annular gap is fully filled with MF. It can be noticed that the Nu can be enhanced by increasing the difference in the inlet temperatures between the hot and cold streams, and the air ratio.

It is noticed that the Nusselt number increases with increasing the (ΔT) as when the temperature difference enlarges the amount of heat transfer increases. Due to the fact that the Nusselt number is a function of heat transfer rate, for the same (AR) values, the reason is that when the value of (ΔT) is high, the heat transfer rate between the two fluids is great, and therefore the values of Nu are high. Notice the value of Nu increasing when the value of (ΔT = 50 C°).

Thus, it can be reported that the heat recovery can be efficient in the cold climates and or when the double-pipe heat exchanger fixed near the exhaust channel. It can be concluded that the optimal ΔT_{in} in this partition (i.e., ΔT_{in} = 50°C) is considered in the all next examined parameters.

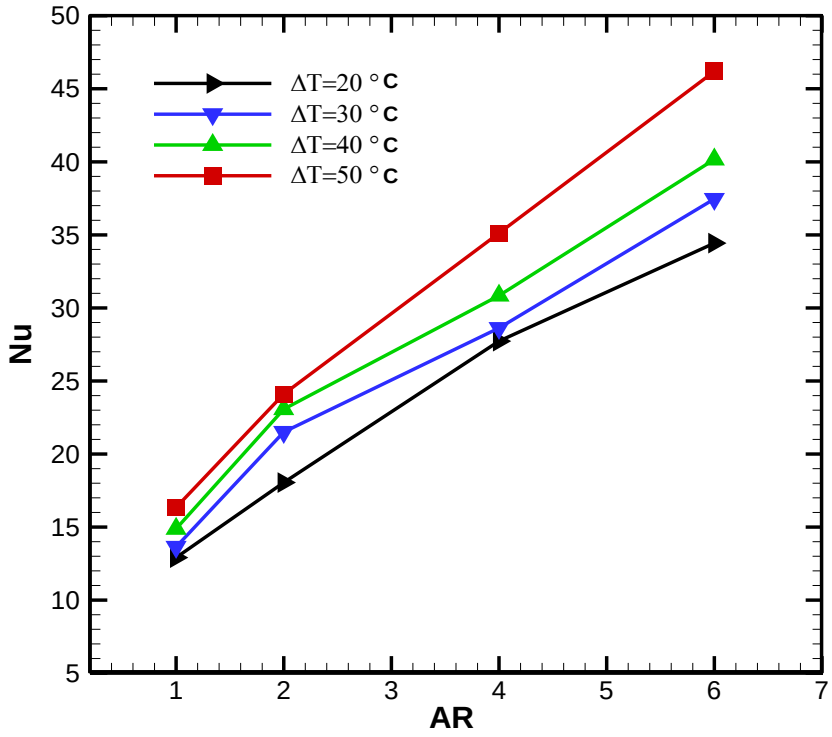

(a)

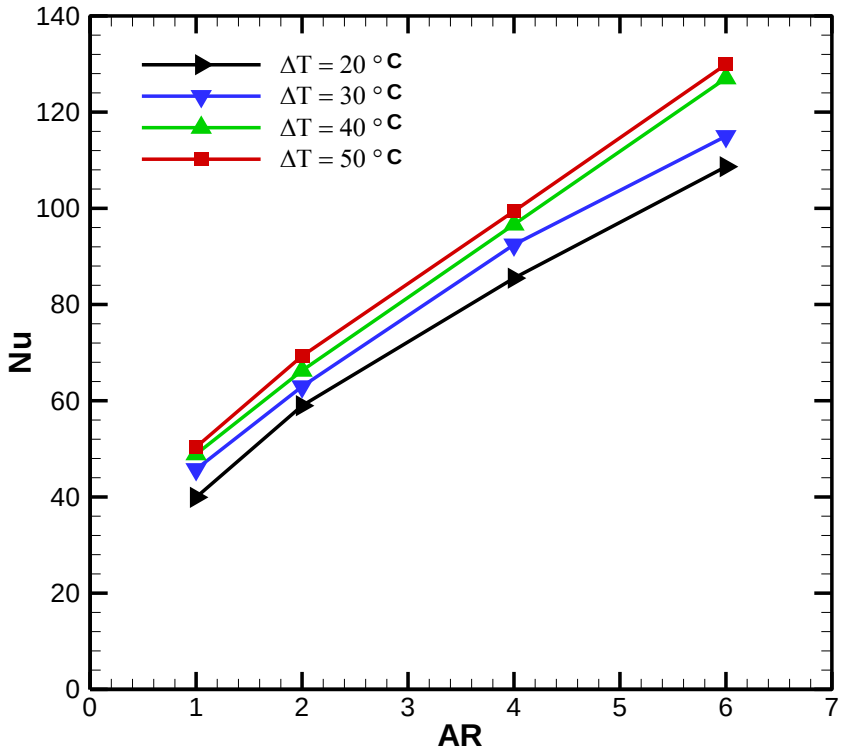

(b)

Figure 0.2 Effect of ΔT in on the average Nusselt number for several values of air ratio; (a) case 8, and (b) case 1.

4.4 Effect of AR on The Heat Transfer

According to Fig. (4.2.a) and Fig. (4.2.b), it can be seen that the parameter of air ratio examination is included as well. The AR has a clear effect on the rate of heat transfer in a double-pipe heat exchanger. It was found that when the increases by keeping (ΔT) constant, the values of heat transfer rate represent by Nusselt number increases. This can be attributed to the fact that when the AR increases the air turbulence inside the cold stream enhances and more mixing between the cold layer and hot layer can be obtained. The enhancement in the Nusselt number was (2.87) and (2.5) for case 8 and 1, respectively, when ΔT = 50 °C.

Because the AR is a range of the air flow rate, therefore, a wide range is covered in this study for focusing on the high Reynolds number. Where it is noticed that the Nusselt values increased at (AR = 6) by 0.39 than the value of (AR = 1) as shown in Fig. (4.2.a) and Fig. (4.2.b).

4.5 Thermal Performance

4.5.1 Local Wall Temperature Distribution

The behavior of the local wall temperature of the outer surface of the copper pipe along the axial length of the test section versus the effect of Reynolds number for case 7 as shown in Fig. (4.3). The reason for this is that the value of the ($\Delta T = T_{h\ in} - T_{c\ in}$) is greater, so the rate of heat transfer is greater. Besides, when increase the Re number lead to more decrease in copper pipe surface temperature. By comparing the behavior lowest and highest Re number, the inlet temperature has a highest difference of 2.8 °C and this difference gradually decreased along copper pipe to be 0.4°C. This behavior due to the high air mixing. By observing the outlet hot air temperatures and the inlet cold air temperatures, it is found that the hot air leaving the test section at a higher temperature than the ambient temperature. The reason is the short

length of the test section and the amount of hot air used in this study. Therefore, the time that the hot air takes is short and not enough to transfer the heat from the hot air to the cold air.

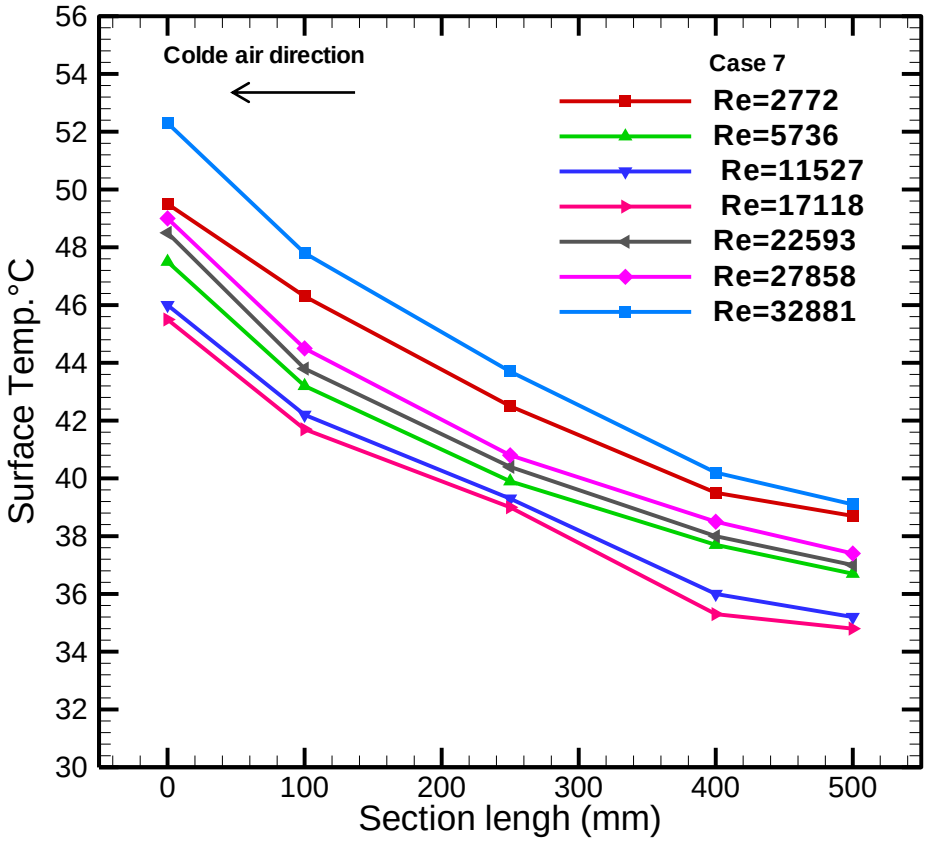

Figure 0.3 Axial wall temperature distribution along the test section.

The effect of the arrangements of the metal foam on the value of ($\Delta T_c = T_{c\,o} - T_{c\,in}$) was clear. The tests that were carried out with the inlet temperature of cold air are different, so the outlet temperature will be different as well, so the explanation of the behavior will be completed as in Fig. (4.4).

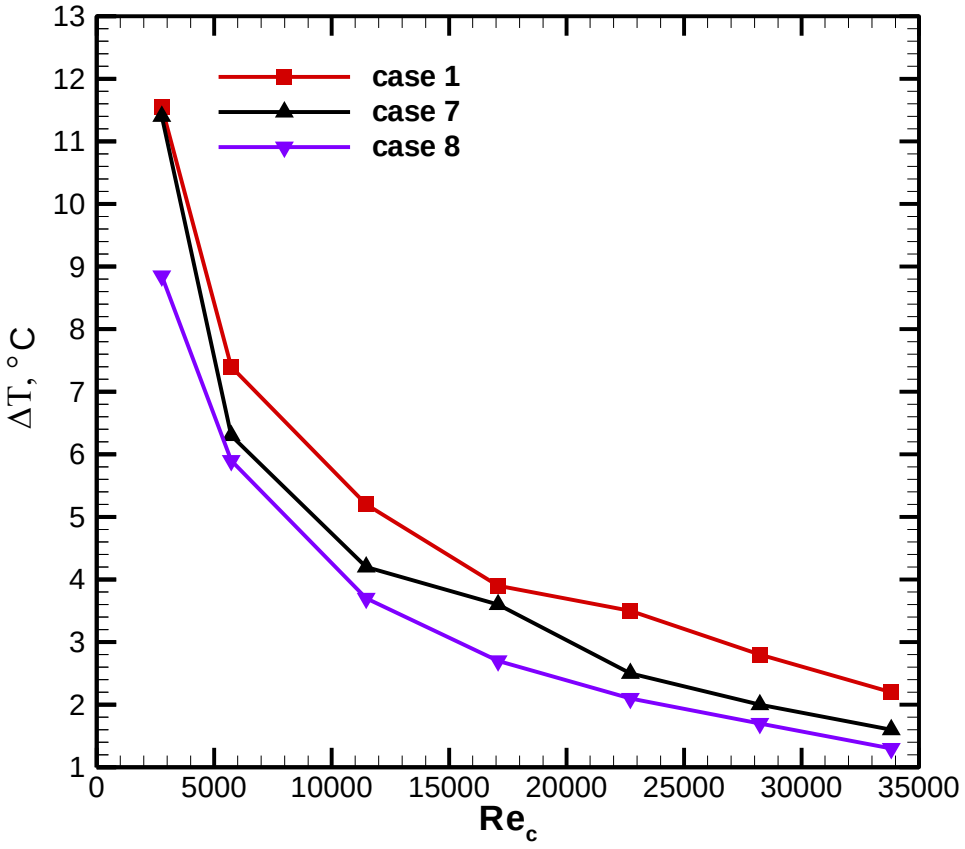

Figure 0.4 Effect of Reynolds number on the (ΔT_c) for case 1, 7, and 8.

4.5.2 Heat Transfer Coefficient

The average convection heat transfer coefficient versus Reynolds number was explained in Fig. (4.5) for all metal foam arrangements, it can be seen that the smooth annulus case 8 shows the lowest heat transfer compared to others. The full filled pattern case 1 provides the highest heat transfer enhancement while the heat transfer of other patterns is lying in between depending on the amount of the metal foam and the ratio of closing the gap passage by metal foam. It was found that the highest value of the heat transfer coefficient was found to be $271.2\ W/m^2.°C$ for case 1 followed by case 7 which was found to be $221.85\ W/m^2.°C$. The lowest value was obtained for the smooth case 8 when h = $86.7\ W/m^2.°C$ at Re = 32,881. It can be also seen that the enhancement in the convection heat transfer coefficient increases with

increasing the Re number due to metal foam caused by high pressure in the inlet.

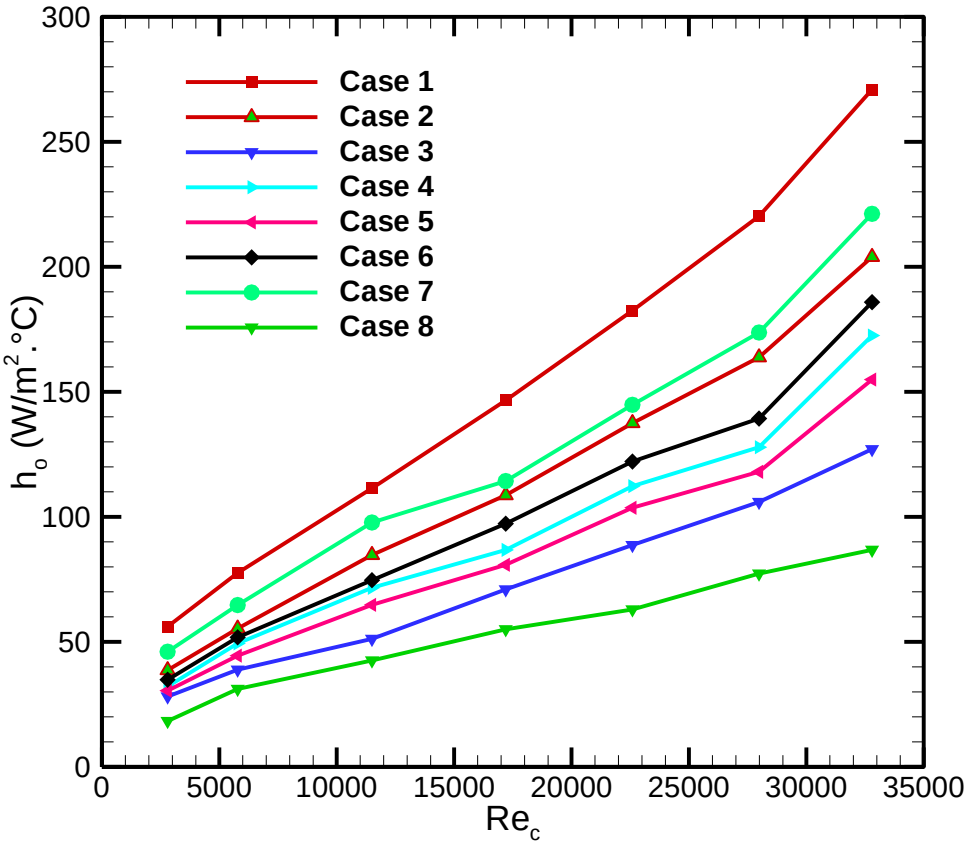

Figure 0.5 Effect of Reynolds number on the convection heat transfer coefficient for several MF arrangements.

4.5.3 Local Nusselt Number

According to experimental work, the local Nusselt number was calculated at points (0,100, 250,400, and 500 mm) from the length of the test section for a constant Reynolds number of (11,500) between the two pipes as shown in Fig.(4.6). It is necessary to say that the position (0 mm) represents the all exit cold stream, while (500 mm) represents the inlet cold stream. It is observed that the highest Nu number is observed at the developing entrance region and it decreases gradually with the flow direction due to the rise in the cold air temperature.

The trend of Nu number is observed in all patterns proposed here, exception case 2 as the MF was fixed at the second half of the channels (from mid-length to the channel exit). In addition, case 6 shows the same trend due to the amount of the MF increases with the flow direction (i.e., the amount of MF at the exit is larger than half at the inlet).

It is clearly to notice that the cases 1, 3, 4, 5, 7, and 8 have the same trend, while case 2 and 6 are different. In case 2, the Nu is high at the stream inlet, but it jumps up at the mid-length due to the MF and then decreases. For case 6, the amount of the MF increases gradually with the cold air direction, and thus, the trend of Nu seems to be constant along the channel length.

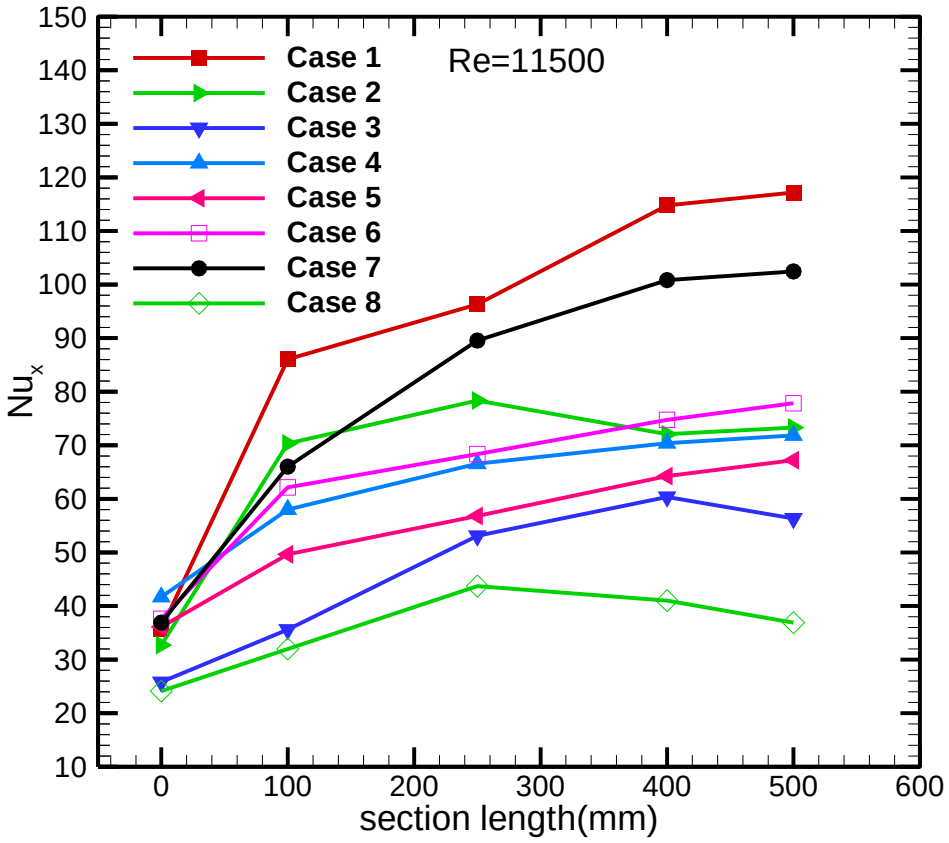

Figure 0.6 Axial local Nusselt number for all patterns.

4.5.4 Average Nusselt Number

The average Nu number is studied in this section with different Re number for all MF arrangements as shown in Fig. (4.7). It was found that the metal foam could increase the heat absorption due to high heat transferred by conduction through the solid edges of the porous matrix and high heat transferred by convection due to increasing the heat transfer surface area between the fluid and solid zone in the porous region. It can be seen that the smooth pattern shows the lowest convective heat transfer, while it increases with increasing Reynolds number.

An enhancement in the heat transfer was observed when the MF was used in the form of case 3 as $D_{MF}/D_{pipe} = 0.75$ (i.e., the MF filled 75% from the gap between the two pipes). This is due to compressibility behavior for the air makes the air passes through the free gap (without MF) because of the low flow resistance. Thus, the convection heat transfer between the air and solid of the porous matrix reduces, but it is still higher than the smooth one.

Further heat transfer enhancement was monitored when the MF is arranged in form of case 5 and 4. It is worthy to be mentioned that case No. 5 filled 62.5%, while case 4 filled 50% by MF. Nevertheless, case 5 provided greater augmentation. It can be attributed to the all MF washers (25 washers) fill the stream gap in case 4, while only (12 washers) fill the stream gap completely. It gives an indication that the convection by case 4 is higher than case 5. On the other hand, the air penetrates in all washers uniformly, while in case 5, the penetration of air is non-uniformly in all washers due to the different diameter ratio to the outer cylinder with respect at the inner cylinder due to different MF density.

Additional heat absorption by the MF was recorded in the case 6. For case 7, it showed that the higher heat transfer compared to case 6, although it filled 57.1% from the total annulus gap compared to 62.5% for case 6.

More augmentation in Nu number observes in case 6 due to gradual increases in the MF amount with axial flow direction, although 25% of the annular channel filled with MF completely (as D_{MF}/D_{pipe}). Moreover, the amount of MF in this case is 62.5%. In addition, the whole outer surface of the copper cylinder is sintered by MF, and thus, the conduction heat transfer is higher compared to the previous cases.

Although case 2 fills 50% from the annular gap, it showed higher Nu number with respect to all aforementioned cases. This is due to the fact that the convection carried out in all zone of the MF, all washers fill the annular gap completely, and the MF was fixed at the second half of the cold stream in which the temperature of the hot stream in its highest value .this behavior can be and understand comprehensively by looking to the local Nu number of this case.

Case 7 provided highest Nu number compared to all other partial filling cases. Nevertheless, this case fills 57.1%, but due to its perfect arrangement optimal heat transfer was obtained.

Doubtless, case 1 provides the greatest Nu number due to full filling of the annular gap, in which higher conduction with the copper cylinder, higher convection heat transfer surface area, and larger amount of the MF compared to all other cases.

From the current results, it can be said that higher heat transfer rate can be obtained by reducing the amount of MF and optimizing the MF arrangement. By keeping the MF volume constant (i.e., case 2 and case 4

and case 5 and case 6), the effect of the MF arrangement can be explained from another view of point. An explicit increase in the Nu number when comparison made between case 5, 6 particularly when Re number increases. Although the number of washers of each diameter ratio is the same, the Nu number of case 6 is higher due to the MF arrangement. The arrangement of MF focused at the downstream end of the cold stream in case 6 where hot stream temperature is high, whereas the MF arrangement of case 5 is distributed uniformly along the cold stream.

The same trend is observed in case 2 and 4, where the MF fills the second- half of the cold stream completely in case 2, while in case 4 the MF arrangement is distributed uniformly along the cold air stream.

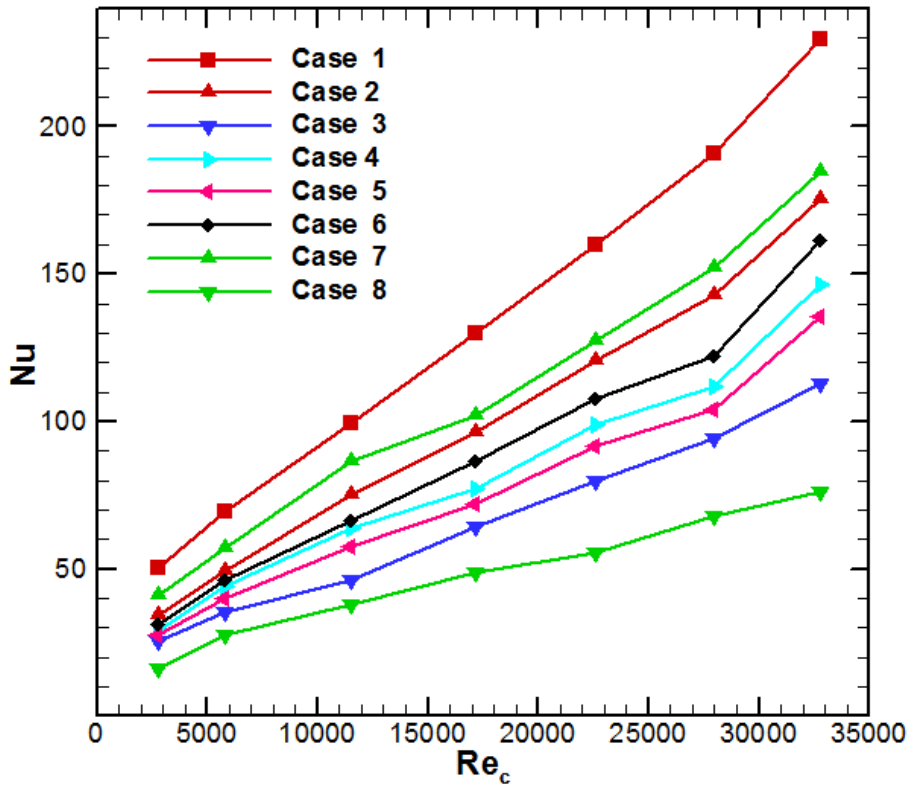

Figure 0.7 The average Nusselt number versus Reynolds number full all MF arrangements.

4.5.5 Effectiveness Of Heat Exchanger

The effectiveness of all cases shown in Fig. (4.8) represents the whole range of Re number. It is observed that the effectiveness increased with increasing the Reynolds number. It was found that the highest effectiveness satisfied in case 1 when the gap between the two pipes is full filled with metal foam, and the lowest effective value is case 8. It is also notice that the effectiveness for case 7 has the best effectiveness compared to all cases in which metal foam is used except for case 1. This is due to the large mixing of cold air entering the gap between the two pipes and to the surface area of contact provided by the metal foam. The maximum and minimum values of effectiveness are 0.637 and 0.564 respectively at Re = 32,881. In general, effectiveness of all cases increases with Re number and unchangeable with the flow rate when Re $\geq$ 16,000. Basically, effectiveness is the lowest for case 8 and increases in case 2, 5. Whereas, case 5 and 3 shows the same effectiveness approximately. This can be called for case 3 and 6 and case 4 and 7. Briefly, case 2 has the same effectiveness of case 5 approximately while it has lower amount of MF. This can be applied for the case 3 and 6, and case 4 and 7. It can be confirmed that higher effectiveness can be obtained by reducing the amount of MF and varying it is arrangement simultaneously.

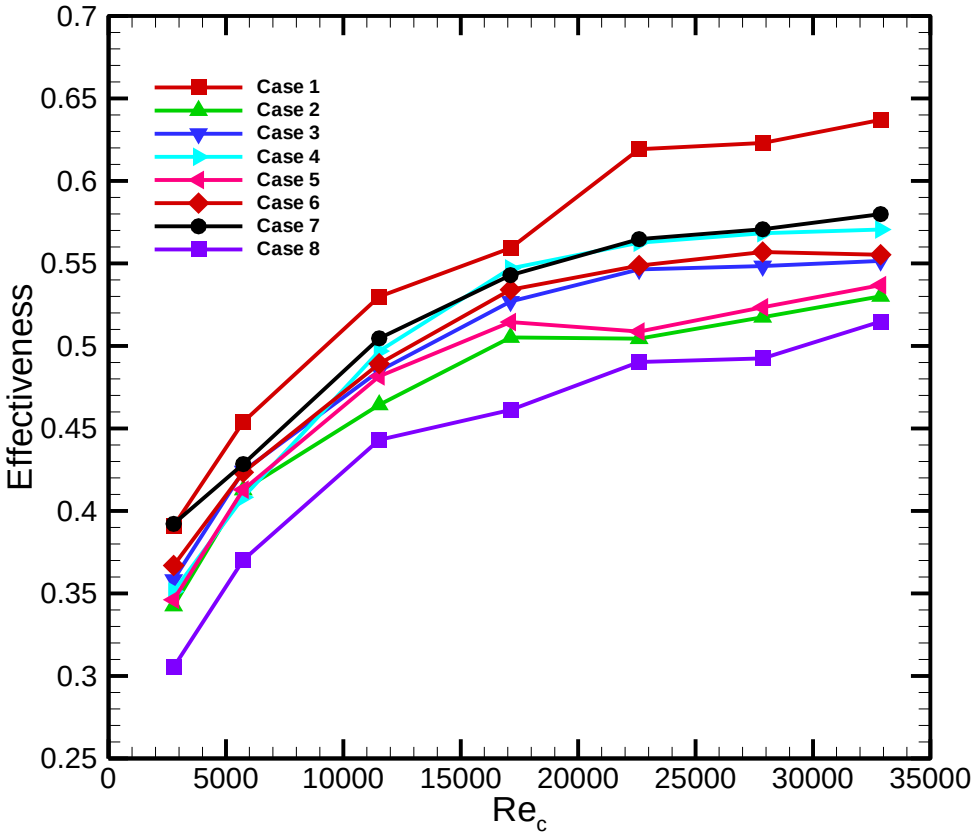

Figure 0.8 The effectiveness of all patterns versus Reynolds number.

4.5.6 Thermal Resistance of the Pipe Wall

Within this analysis, it is noticed that the empty annular Channel exhibits higher Rth, while the lowest R_{th} is observed for full filled heat exchanger. Case 7 show an R_{th} in between. At 0.0008 m^3/s, the R_{th} reduces from 2.71 $℃/W$ to 1.81 $℃/W$ when the empty annular channel is filled completely with MF. The reduction in R_{th} is from 1.45 $℃/W$ to 1.04 $℃/W$ for the same above cases at 0.01 m^3/s. By using the following equation for estimating the reduction ratio in the R_{th}

$$\text{reduction ratio} = \frac{R_{th-full} - R_{th-empty}}{R_{th-full}} \times 100\ \% \qquad (4.1)$$

It is observed the Rth reduction obtained is 33.2% and 28.2% at lowest and highest flow rate, respectively. As shown in Fig. (4.9)

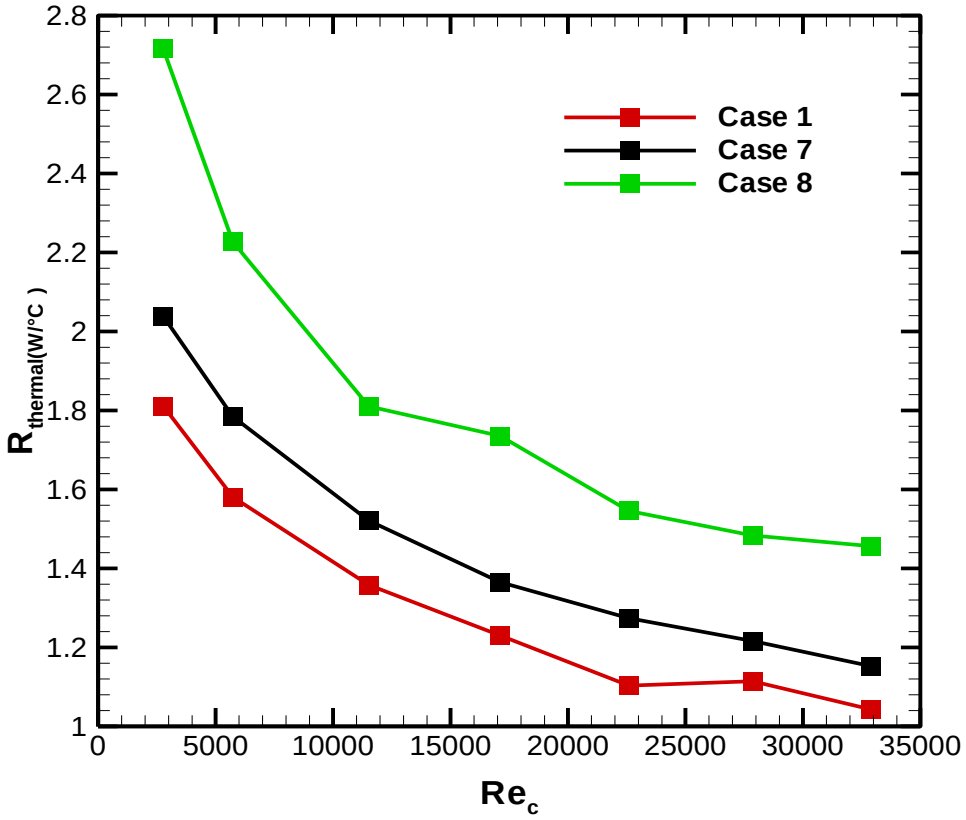

Figure 0.9 The variation of thermal resistance (Rth) with volumetric flow rate.

4.6 Hydraulic Performance

4.6.1 Pressure Drop

The pressure drop across the cold air stream is depicted for all cases over the whole range of the Re number as shown in Fig. (4.10). A small pressure drop which can be neglected as explained in case 8. Higher pressure drop is observed in case 3. Although the MF of case 3 occupies 75% from the annular gap, it shows the lowest pressure drop penalty because the $D_{MF}/D_{pipe} = 0.75$, the air passes through the clear region instead of MF region. More pressure drop penalty is observed by case 7, although the MF occupies 57.1% but 7 MF washers fill the gap completely. Then case 5 and 6 (62.5% filled by MF) exhibit additional flow resistance. Nevertheless, case 6 shows higher ΔP compared to

cases. In case 4 and 2 when 50% of the annular gap is filled with MF, it was seen that more pressure drop compared to all the aforementioned patterns. The highest flow resistance was observed in case 1 in which the air was obliged to flow in MF zone.

4.6.2 Friction Factor

The same trend observed in the pressure drop of all cases was almost repeated in the friction factor. In general, the friction factor drops dramatically at increases Re number, while it becomes stable and unchangeable when Re ≥ 12,000 .The average increase in the $(\frac{f_{MF}}{f_{empty}})$ is observed to be (15.67) for case 2 (the higher frictional losses in the partial filled case). Where the full filled case (case 1) exhibits a rise in the $(\frac{f_{MF}}{f_{empty}})$ about (29.34). While the ratio of $(\frac{f_{case\ 2}}{f_{case\ 1}})$ equals to 0.534 as shown in Fig.(4.11) .

.

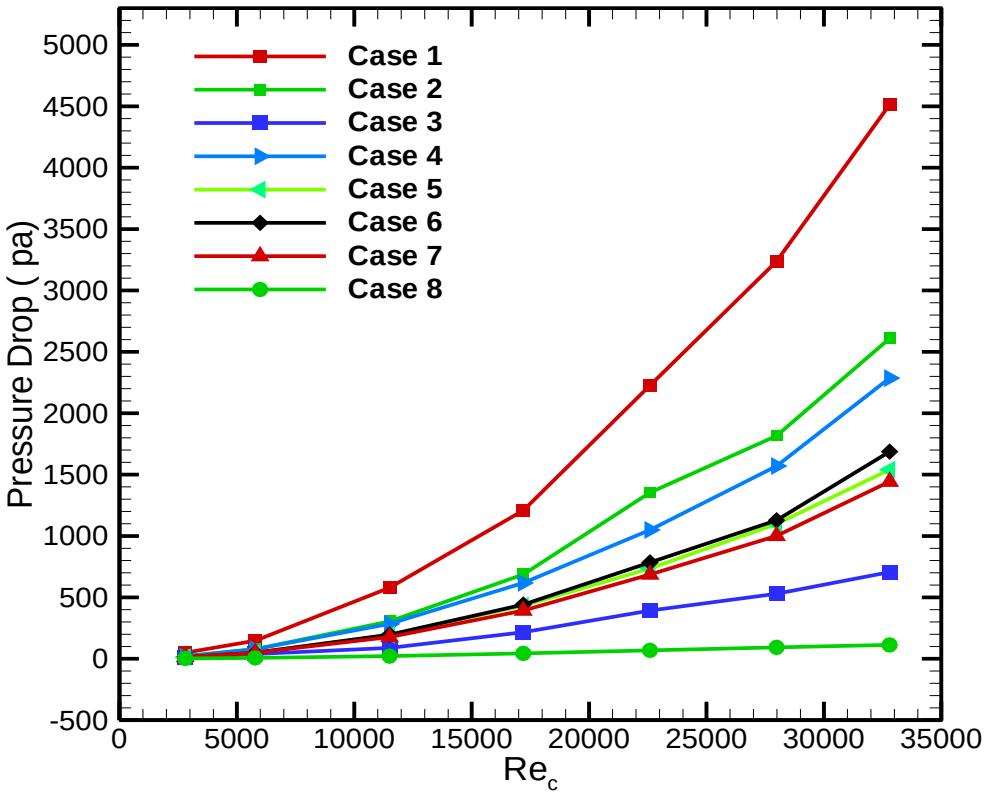

Figure 0.10 The variation of presser drop with Reynolds number.

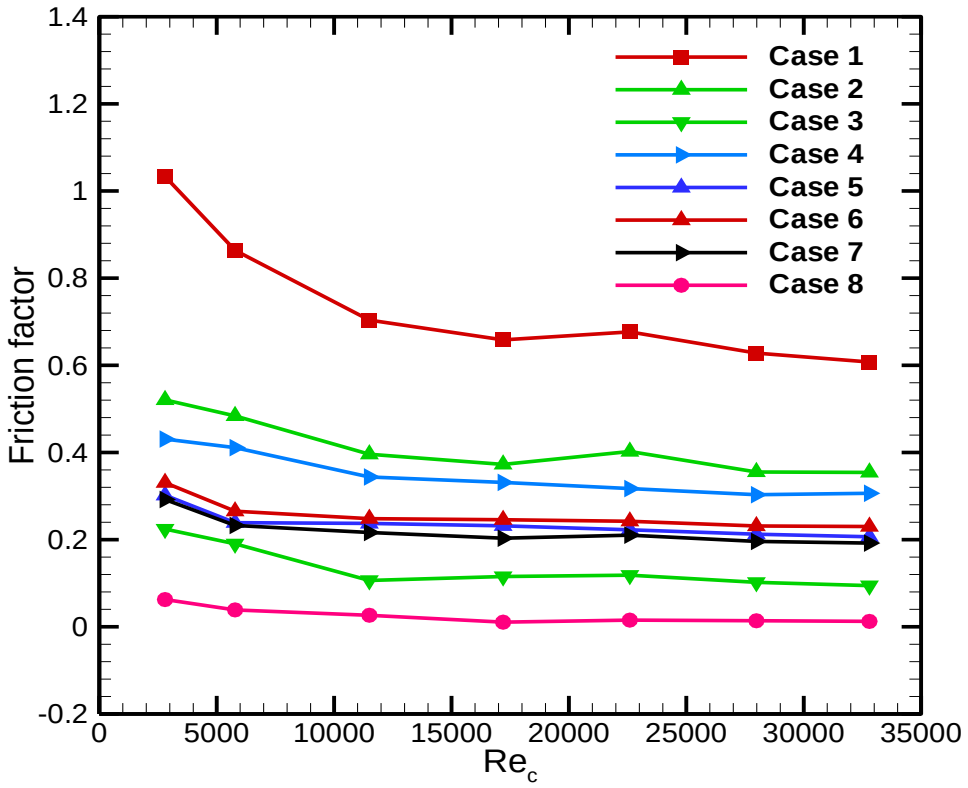

Figure 0.11 The variation of friction factor with Reynolds number

4.7 Performance Evaluation Criteria (PEC)

For a fair comparison between the enhancement in the heat transfer and the increase in the pressure drop, the PEC versus Reynolds number is depicted as shown in Fig. (4.12). Worth to mention that the PEC less than unity represents negative hydro-thermal design as the improvement in the pressure drop is higher than the heat transfer augmentation, and vice versa. It can be seen that, the most cases are lower than unity due to high additional pumping power. It can be said that if the pressure drop is not meter because the heat transfer is the vital role, the low PEC can be taken in to the design considerations. Otherwise, only the PEC greater than one must be considered.

It can be observed that the lowest PEC is in case 4. This case shows moderate increase in the Nu number and moderate increase in the friction loss. The same trend is provided by case 5. Case 3 provides lower enhancement in the Nu number but so small friction factor, therefore, it provided higher PEC compared to the above cases. Creator PEC is also observed in case 2 due to high Nu, moderate friction factor. The PEC of case 2, 6, and 1 are close to each other. Although case 1 provides higher Nu number, it also provides higher pressure drop. A significant increase in the PEC is observed for case 7. This case shows the highest Nu compered to all cases filled partially with MF. All cases show PEC ≥ 1 at low vales of Re number.

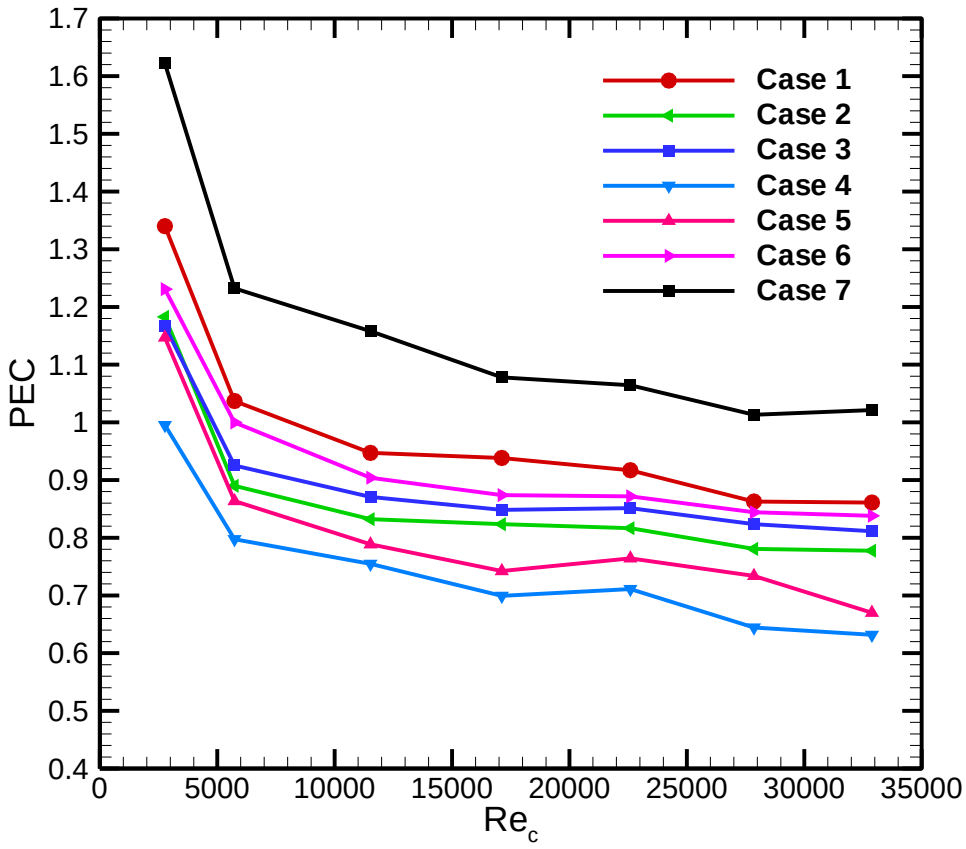

Figure 0.12 The variation of performance evaluated criteria with Reynolds number.

4.8 Research Contribution

To sum up, the heat transfer rate can be strongly improved by using the metal foam in the cold stream side. This heat transfer enhancement could increase the outlet cold air temperature. It means that low fuel is required for heating the air in the combustion chamber of the power plant due to raising the temperature by using the proposed heat recovery design.

In addition, the heat transfer enhancement techniques used could increase the intake air temperature of the chamber same or better than that done be using solid fins. It means low weight is added to the double-pipe heat exchanger when the MF is used instead of fins. Low weight might mean small required material and low cost. The maximum

difference obtained in the cold air temperature was about 11.4 ^{o}C for case 1 at Re 2800.

Moreover, this research adds a significant contribution to the knowledge as it is well-known that when the volume of the MF increases the heat transfer increases, and vice versa. In this research, it is proved that the heat transfer can be improved remarkably simultaneously with reducing the size of the MF used. This main finding in this research differs what was known on the metal foam. From the point of the metal cost view, the material saving obtained here is about 24% when case 7 is used instead of case 3. More details can be extracted from Table 4.2 shown below.

The benefit of material saving, material cost, and temperature rising of the chamber inlet could make the investigators ignore the undesirable increase in the pressure drop due to using MF.

Table 0-1 Arrangement of the MF configuration according to the highest-Nu.

Case (MF)	MF %	rearrangement according case to Nu	MF%	Pressure drop	PEC
1	100	1	100	1	7
3	75	7	57	2	1
5	62.5	2	50	4	6
6	62.5	6	62.5	6	3
7	57	4	50	5	2
2	50	5	62.5	7	5
4	50	3	75	3	4
8	0.0	8	0.0	8	

CHAPTER FIVE
CONCLUSIONS AND RECOMMENDATIONS

5.1 Conclusions

In this experimental study using metal foam 15PPI with porosity of 0.95 at different configuration and arrangement has been reported. The metal foam was installed on the outer surface of the inner pipe, through the gap between the two pipes. The effect of metal foam on the heat transfer rate and pressure drop in the exchanger is evaluated. The results that obtained by this study can be summarized:

1- The Nu number increased with increasing ΔT. The higher Nu was with ΔT= 50 C°.
2- The Nu number increased linearly when AR increased.
3- Case 7 showed the optimal heat transfer compared to all other partial filling MF cases. The full filling with MF still outperforms for all cases.
4- Case 3 showed lower friction loss due to D_{MF}/D_{pipe} = 0.75. The highest friction factor was observed in case 1 due to full filling with MF. With increase Reynolds number, the friction factor decreases. Where the highest value of friction factor was in case 1 (f= 1.033) and the lowest value in case 8 equal (f = 0.0833) at Re =2800.
5- The optimal PEC is seen for case 7 (PEC = 1.62 at Re = 2800). All others cases showed PEC > 1 only at low Re number.
6- Focusing the MF matrix to be the second-half of the cold air stream.
7- In general it can be said although the Nu and friction factor increase with increasing the amount of MF, the Nu can be increased with moderate increase in the friction factor by optimizing the arrangement of MF. Two essential parameters play an important role in increasing

PEC; The MF diameter and the MF distribution along the axial length of the cold stream.

5.2 Recommendations

The following aspects are suggested for future researches.

i. Repeat the study with the use of MF at different characteristics such as 5PPI, 20PPI, and so on.
ii. Using other geometric shapes from MF.
iii. Changing the amount of hot air and evaluating the effect on the thermal performance values.
iv. Increasing the length of the test section and calculating its effect on the general performance of the heat exchange.
v. The working fluid may be using hot water instead of hot air and studying its effect on the general performance of the exchanger.

REFERENCES

[1] R. Thejaraju, K. B. Girisha, S. H. Manjunath, and B. S. Dayananda, "Experimental investigation of turbulent flow behavior in an air to air double pipe heat exchanger using novel para winglet tape," *Case Stud. Therm. Eng.*, vol. 22, no. December, p. 100791, 2020, doi: 10.1016/j.csite.2020.100791.

[2] S. P. Govindani, "Experimental Analysis of Heat Transfer Enhancement in a Double Pipe Heat Exchanger Using Inserted Rotor Assembled Strand," Volume: 03 Issue: 01 | Jan-2016.

[3] Nihad Dukau, *Metal foams;Fundametals and Applications*. 2013.

[4] N. Targui and H. Kahalerras, "Analysis of fluid flow and heat transfer in a double pipe heat exchanger with porous structures," *Energy Convers. Manag.*, vol. 49, no. 11, pp. 3217–3229, 2008, doi: 10.1016/j.enconman.2008.02.010.

[5] A. Nasser, Adel Alhusseny and A. Turan, "Rotating metal foam structures for performance enhancement of double-pipe heat exchangers," *Int. J. Heat Mass Transf.*, vol. 105, pp. 124–139, 2017, doi: 10.1016/j.ijheatmasstransfer.2016.09.055.

[6] T. L. Bergman, F. P. Incropera, D. P. DeWitt, and A. S. Lavine, *Fundamentals of heat and mass transfer*. John Wiley & Sons, 2011.

[7] S. Chikh and N. Allouache, "Optimal performance of an annular heat exchanger with a porous insert for a turbulent flow," *Appl. Therm. Eng.*, vol. 104, pp. 222–230, 2016, doi: 10.1016/j.applthermaleng.2016.05.069.

[8] S. T. W. Kuruneru, K. Vafai, E. Sauret, and Y. T. Gu, "Application of porous metal foam heat exchangers and the implications of particulate fouling for energy-intensive industries," *Chem. Eng. Sci.*, vol. 228, 2020, doi: 10.1016/j.ces.2020.115968.

[9] Bergles , A.E, *Techniques to Augment.Heat Transfer,*. 1985.

[10] M. P. Orihuela, F. Shikh Anuar, I. Ashtiani Abdi, M. Odabaee, and K. Hooman, "Thermohydraulics of a metal foam-filled annulus," *Int. J. Heat Mass Transf.*, vol. 117, pp. 95–106, 2018, doi: 10.1016/j.ijheatmasstransfer.2017.10.009.

[11] O. T. Fadhil, H. E. Ahmed, and W. A. Salih, " Effect of Grooves Geometric Parameters on Hydraulic Thermal Performance of Circular Pipe Partially Filled with Metallic Foam," "Anbar Journal Of Engineering Science © vol. 7, pp. 382–394.

[12] S. Rashidian and M. R. Tavakoli, "Using Porous Media to Enhancement of Heat Transfer in Heat Exchangers," *Int. J. Adv. Eng. Manag. Sci.*, vol. 3, no. 11, pp. 1051–1064, 2017, doi: 10.24001/ijaems.3.11.5.

[13] J. A. Hamzah and M. A. Nima, "Experimental Study of Heat Transfer Enhancement in Double-Pipe Heat Exchanger Integrated with Metal Foam Fins," *Arab. J. Sci. Eng.*, vol. 45, no. 7, pp. 5153–5167, 2020, doi: 10.1007/s13369-020-04371-3.

[14] E. F. Abbas, S. R. Aslan, and T. A. Ridha, "Experimental Investigation of Heat Transfer Enhancement Methods on the Thermal Performance of Double Pipe Heat Exchanger," *International Journal of Engineering Research & Technology (IJERT)* vol.6, no. 09, pp.169-174, 2017).

[15] I. W. Maid, K. H. Hilal and J. K. Hassun, "Experimental Study Of Heat Transfer Enhancement In Heat Exchanger Using Porous Media," *Global Journal of Engineering Science and Research Management*, vol. 4, no. 9, pp. 82–91, 2017, doi: 10.5281/zenodo.886915.

[16] M. Mishra, and U. K Nayak, "Experimental Investigations of Double Pipe Heat Exchanger With Triangular Baffles," *Int. Res. J.*

Eng. Technol., vol. 03, no. 08, pp. 1137–1141, 2016.

[17] K. Nawaz, J. Bock, and A. M. Jacobi, "Thermal-hydraulic performance of metal foam heat exchangers under dry operating conditions," *Appl. Therm. Eng.*, vol. 119, pp. 222–232, 2017, doi: 10.1016/j.applthermaleng.2017.03.056.

[18] A. A. Sertkaya, K. Altinisik, and K. Dincer, "Experimental investigation of thermal performance of aluminum finned heat exchangers and open-cell aluminum foam heat exchangers," *Exp. Therm. Fluid Sci.*, vol. 36, pp. 86–92, 2012, doi: 10.1016/j.expthermflusci.2011.08.008.

[19] M. Sheikholeslami, M. Gorji-Bandpy, and D. D. Ganji, "Experimental study on turbulent flow and heat transfer in an air to water heat exchanger using perforated circular-ring," *Exp. Therm. Fluid Sci.*, vol. 70, pp. 185–195, 2016, doi: 10.1016/j.expthermflusci.2015.09.002.

[20] H. Kahalerras and N. Targui, "Numerical analysis of heat transfer enhancement in a double pipe heat exchanger with porous fins," *Int. J. Numer. Methods Heat Fluid Flow*, vol. 18, no. 5, pp. 593–617, 2008, doi: 10.1108/09615530810879738.

[21] X. Chen, X. Xia, C. Sun, F. Wang, and R. Liu, "Performance evaluation of a double-pipe heat exchanger with uniform and graded metal foams," *Heat Mass Transf. und Stoffuebertragung*, vol. 56, no. 1, pp. 291–302, 2020, doi: 10.1007/s00231-019-02700-3.

[22] H. Moghadasi, E. Aminian, H. Saffari, M. Mahjoorghani, and A. Emamifar, "Numerical analysis on laminar forced convection improvement of hybrid nanofluid within a U-bend pipe in porous media," *Int. J. Mech. Sci.*, vol. 179, no. March, p. 105659, 2020, doi: 10.1016/j.ijmecsci.2020.105659.

[23] M. Benmerkhi, M. Afrid, and D. Groulx, “Thermally developing forced convection in a metal foam-filled elliptic annulus,” *Int. J. Heat Mass Transf.*, vol. 97, pp. 253–269, 2016, doi: 10.1016/j.ijheatmasstransfer.2016.02.017.

[24] A. Jamarani, M. Maerefat, N. F. Jouybari, and M. E. Nimvari, “Thermal Performance Evaluation of a Double-Tube Heat Exchanger Partially Filled with Porous Media Under Turbulent Flow Regime,” *Transp. Porous Media*, vol. 120, no. 3, pp. 449–471, 2017, doi: 10.1007/s11242-017-0933-x.

[25] H. R. Abbasi, E. Sharifi Sedeh, H. Pourrahmani, and M. H. Mohammadi, “Shape optimization of segmental porous baffles for enhanced thermo-hydraulic performance of shell-and-tube heat exchanger,” *Appl. Therm. Eng.*, vol. 180, p. 115835, 2020, doi: 10.1016/j.applthermaleng.2020.115835.

[26] M. Odabaee and K. Hooman, “Application of metal foams in air-cooled condensers for geothermal power plants: An optimization study,” *Int. Commun. Heat Mass Transf.*, vol. 38, no. 7, pp. 838–843, 2011, doi: 10.1016/j.icheatmasstransfer.2011.03.028.

[27] N. I. Ibrahim, F. A. Al-Sulaiman, S. Rahman, B. S. Yilbas, and A. Z. Sahin, “Heat transfer enhancement of phase change materials for thermal energy storage applications: A critical review,” *Renew. Sustain. Energy Rev.*, vol. 74, no. October 2015, pp. 26–50, 2017, doi: 10.1016/j.rser.2017.01.169.

[28] H. J. Xu, Z. G. Qu, and W. Q. Tao, “Numerical investigation on self-coupling heat transfer in a counter-flow double-pipe heat exchanger filled with metallic foams,” *Appl. Therm. Eng.*, vol. 66, no. 1–2, pp. 43–54, 2014, doi: 10.1016/j.applthermaleng.2014.01.053.

[29] H. Arasteh, M. R. Salimpour, and M. R. Tavakoli, “Optimal

distribution of metal foam inserts in a double-pipe heat exchanger," *Int. J. Numer. Methods Heat Fluid Flow*, vol. 29, no. 4, pp. 1322–3142, 2019, doi: 10.1108/HFF-04-2018-0162.

[30] C. Y. Zhao, W. Lu, and S. A. Tassou, "Thermal analysis on metal-foam filled heat exchangers. Part II: Tube heat exchangers," *Int. J. Heat Mass Transf.*, vol. 49, no. 15–16, pp. 2762–2770, 2006, doi: 10.1016/j.ijheatmasstransfer.2005.12.014.

[31] T. Zhao. H. Tian, L. Shi, T. Chen. X Ma, "Numerical analysis of flow characteristics and heat transfer of high-temperature exhaust gas through porous fins," *Appl. Therm. Eng.*, vol. 165, 2020, doi: 10.1016/j.applthermaleng.2019.114612.

[32] B. I. Pavel and A. A. Mohamad, "An experimental and numerical study on heat transfer enhancement for gas heat exchangers fitted with porous media," *Int. J. Heat Mass Transf.*, vol. 47, no. 23, pp. 4939–4952, 2004, doi: 10.1016/j.ijheatmasstransfer.2004.06.014.

[33] X. Chen, F. Tavakkoli, and K. Vafai, "Analysis and characterization of metal foam-filled double-pipe heat exchangers," *Numer. Heat Transf. Part A Appl.*, vol. 68, no. 10, pp. 1031–1049, 2015, doi: 10.1080/10407782.2015.1031607.

[34] M. K. Alkam and M. A. Al-Nimr, "Improving the performance of double-pipe heat exchangers by using porous substrates," *Int. J. Heat Mass Transf.*, vol. 42, no. 19, pp. 3609–3618, 1999, doi: 10.1016/S0017-9310(99)00033-2.

[35] N. Targui and H. Kahalerras, "Analysis of a double pipe heat exchanger performance by use of porous baffles and pulsating flow," *Energy Convers. Manag.*, vol. 76, pp. 43–54, 2013, doi: 10.1016/j.enconman.2013.07.022.

[36] T. Edition and R. W. Sebesta, "Instructor's Solutions Manual," 2013.

[37] S. J. Kline, “Describing uncertainty in single sample experiments,” *Mech. Eng.*, vol. 75, pp. 3–8, 1953.

Appendix A

Thermocouples Calibration

The thermocouples were calibrated with a mercury thermometer, and the amount of error in each thermocouple in the readings was adjusted (adding or decreasing) through a feature that was characterized by the screens (Digital Temperature controller) that show the readings that have been installed in the device used. In addition, a second reference thermocouple devices was carried out by the laboratories of the Standardization and Quality Control Department / Ministry of Planning, and the results showed the accuracy of the readings as shown in Figure (3.13) where the x-axis represents the reference of temperatures that were adopted for calibration and the y-axis represents the readings of thermocouple.

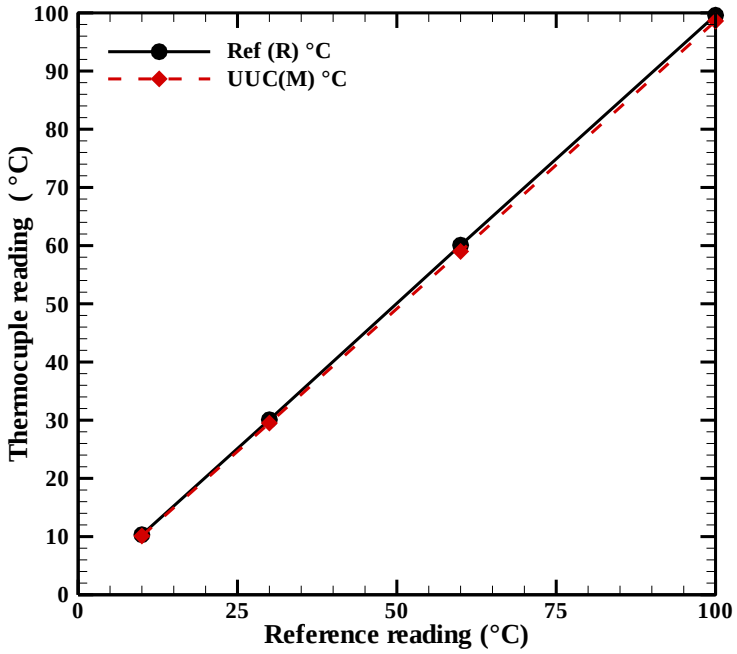

A.1: Calibration of thermocouple carried out by SQCD /ministry of planning.

Appendix B

Uncertainty Analysis

B.1 Uncertainty of Key Parameters

The uncertainties of key various parameters are presented in follow table.

Table B.1 The primary uncertainties for various parameters.

NO.	Variable	Uncertainty
1	The length of channel, L	$\pm$1.0 mm
2	The inner diameter of inner pipe , d_i	$\pm$0.1 mm
3	The outer diameter of inner pipe , d_o	$\pm$0.1 mm
4	The inner diameter of outer pipe , D_i	$\pm$0.1 mm
5	Inlet cold air temperature, $T_{c,in}$	$\pm$0.93%
6	outlet cold air temperature, $T_{c,o}$	$\pm$0.93%
7	Inlet hot air temperature, $T_{h,in}$	$\pm$0.93%
8	outlet hot air temperature, $T_{h,o}$	$\pm$0.93%
9	Surface temperature, T_s	$\pm$0.93%
10	flow rate,	$\pm$5.0%
11	Pressure drop, Δp	6.5%

B.2 Uncertainty of Hydraulic Diameter

The hydraulic diameter was displayed in equation 4.5 as follows:

$$D_h = D_i - d_o \tag{B.1}$$

The uncertainty of hydraulic diameter is expressed by:

$$U_{D_h} = \pm\sqrt{\left(\frac{\partial D_h}{\partial D_i}U_{D_i}\right)^2 + \left(\frac{\partial D_h}{\partial d_o}U_{d_o}\right)^2} \tag{B.2}$$

Where

$$\frac{\partial D_h}{\partial D_i} = 1 \tag{B.3}$$

$$\frac{\partial D_h}{\partial d_o} = -1 \tag{B.4}$$

Substitute this values in equation B.2 as follows:

$$U_{D_h} = \pm\sqrt{\left(U_{D_i}\right)^2 + \left(U_{d_o}\right)^2} \tag{B.5}$$

Substitute the value of D_i and d_o from Table B.1 in above equation expresses:

$$U_{D_h} = \pm\sqrt{(0.1)^2 + (0.1)^2} = \pm 0.141\ mm \tag{B.6}$$

Furthermore, the relative uncertainty is determined as follows:

$$\frac{U_{D_h}}{D_h} = \pm\frac{0.141}{23} = \pm 0.6\ \% \tag{B.7}$$

B.3 Uncertainty of Cross Sectional Area

The cross-sectional area was:

$$A_c = \frac{\pi {D_h}^2}{4} \tag{B.8}$$

And the cross sectional area uncertainty (A_c) is computed as follows:

$$U_{A_c} = \pm \frac{1}{A_c} \sqrt{\left(\frac{\partial A_c}{\partial D_h} U_{D_h}\right)^2} \tag{B.9}$$

Where

$$\frac{\partial A_c}{\partial D_h} = \frac{\pi D_h}{2} = \frac{2A_c}{D_h} \tag{B.10}$$

Substitute the above terms in equation B.9 as follows:

$$U_{A_c} = \pm \sqrt{\left(\frac{2U_{D_h}}{D_h}\right)^2} \tag{B.12}$$

$$= \pm \sqrt{\left(\frac{2 * 0.141}{23}\right)^2} = \pm 0.0123\ mm^2 \tag{B.13}$$

The relative uncertainty of A_c is obtained as follows:

$$\frac{U_{A_c}}{A_c} = \pm \frac{0.0123}{415.26}$$

$$= \pm 0.003\ \% \tag{B.14}$$

B.4 Uncertainty of Surface Area

The outer surface area of the inner pipe is given as:

$$A_s = \pi d_o L \tag{B.15}$$

The relative uncertainty of A_S is evaluated as follows:

$$\frac{U_{A_s}}{A_s} = \pm \frac{1}{A_S} \sqrt{\left(\frac{\partial A_s}{\partial d_o} U_{d_o}\right)^2 + \left(\frac{\partial A_s}{\partial L} U_L\right)^2} \tag{B.16}$$

Here,

$$\frac{\partial A_s}{\partial d_o} = \frac{A_s}{d_o} \tag{B.17}$$

$$\frac{\partial A_s}{\partial L} = \frac{A_s}{L} \tag{B.18}$$

Substituting the above terms in equation B.16 gives:

$$\frac{U_{A_s}}{A_s} = \pm \sqrt{\left(\frac{U_{d_o}}{d_o}\right)^2 + \left(\frac{U_L}{L}\right)^2} \tag{B.19}$$

$$= \pm \sqrt{\left(\frac{0.1}{19}\right)^2 + \left(\frac{1}{500}\right)^2} = \pm 0.563\% \tag{B.20}$$

B.5 Uncertainty of Reynolds Number

Reynolds number can be expressed as follows:

$$Re = \frac{4\dot{m}}{\pi D_h \mu_c} \tag{B.21}$$

The Reynolds number uncertainty is presented as follows:

$$U_{Re} = \pm\sqrt{\left(\frac{\partial Re}{\partial \dot{m}} U_{\dot{m}}\right)^2 + \left(\frac{\partial Re}{\partial D_h} U_{D_h}\right)^2} \quad (B.22)$$

Where,

$$\frac{\partial Re}{\partial \dot{m}} = \frac{4}{\pi D_h \mu_c} = \frac{Re}{\dot{m}} \quad (B.23)$$

$$\frac{\partial Re}{\partial D_h} = \frac{-4\dot{m}}{\pi {D_h}^2 \mu_c} = \frac{-Re}{D_h} \quad (B.24)$$

Substituting these terms in equation B.22, thus, the relative uncertainty of Reynolds number is presented as:

$$\frac{U_{Re}}{Re} = \pm\sqrt{\left(\frac{U_{\dot{m}}}{\dot{m}}\right)^2 + \left(\frac{U_{D_h}}{D_h}\right)^2} \quad (B.25)$$

$$= \pm\sqrt{\left(\frac{0.000567}{0.01134}\right)^2 + \left(\frac{0.141}{23}\right)^2} = \pm 5.037\% \quad (B.26)$$

B.6 Friction Factor Uncertainty

The friction factor was expressed as follows:

$$f = \frac{2\Delta p\ \rho\ A_c^2}{\dot{m}^2} \frac{D_h}{L} \quad (B.27)$$

The friction factor uncertainty is as shown by:

$$U_f = \pm \sqrt{\begin{matrix}\left(\frac{\partial f}{\partial \Delta p} U_{\Delta p}\right)^2 + \left(\frac{\partial f}{\partial \dot{m}} U_{\dot{m}}\right)^2 + \left(\frac{\partial f}{\partial A_c} U_{A_c}\right)^2 \\ + \left(\frac{\partial f}{\partial D_h} U_{D_h}\right)^2 + \left(\frac{\partial f}{\partial L} U_L\right)^2\end{matrix}} \quad \text{(B.28)}$$

Where

$$\frac{\partial f}{\partial \Delta p} = \frac{2\rho A_c^2}{\dot{m}^2} \frac{D_h}{L} = \frac{f}{\Delta p} \quad \text{(B.29)}$$

$$\frac{\partial f}{\partial \dot{m}} = \frac{-4}{\dot{m}} \frac{\Delta p \, \rho \, A_c^2}{\dot{m}^2} \frac{D_h}{L} = \frac{-2}{\dot{m}} f \quad \text{(B.30)}$$

$$\frac{\partial f}{\partial A_c} = \frac{4\Delta p \, \rho \, A_c}{\dot{m}^2} \frac{D_h}{L} = \frac{2}{A_c} f \quad \text{(B.31)}$$

$$\frac{\partial f}{\partial \, D_h} = \frac{2\Delta p \, \rho \, A_c^2}{\dot{m}^2} \frac{1}{L} = \frac{f}{D_h} \quad \text{(B.32)}$$

$$\frac{\partial f}{\partial L} = \frac{-2\Delta p \, \rho \, A_c^2}{\dot{m}^2} \frac{D_h}{L} = \frac{-f}{L} \quad \text{(B.33)}$$

Substituting above terms in equation B.28, thus, the relative uncertainty of friction factor is expressed by:

$$\frac{U_f}{f} = \pm \sqrt{\left(\frac{U_{\Delta p}}{\Delta p}\right)^2 + \left(\frac{-2U_{\dot{m}}}{\dot{m}}\right)^2 + \left(\frac{2U_{A_c}}{A_c}\right)^2 + \left(\frac{U_{D_h}}{D_h}\right)^2 + \left(\frac{-U_L}{L}\right)^2} \quad \text{(B.34)}$$

$$\frac{U_f}{f} = \pm \sqrt{\begin{matrix}\left(\frac{89.271}{1373.4}\right)^2 + \left(\frac{-2 * 0.000567}{0.01134}\right)^2 + \left(\frac{2 * 0.0123}{415.26}\right)^2 \\ + \left(\frac{0.141}{23}\right)^2 + \left(\frac{1.0}{500}\right)^2\end{matrix}}$$

$$= \pm 11.944\% \quad \text{(B.35)}$$

B.7 Uncertainty in Q_c

The heat received by cold fluid was displayed given by:

$$Q_c = \dot{m}\, C_{p,c}\, (T_{c,o} - T_{c,i}) \tag{B.36}$$

The uncertainty of Q_c is achieved by:

$$U_{Q_c} = \pm \sqrt{\left(\frac{\partial Q_c}{\partial \dot{m}} U_{\dot{m}}\right)^2 + \left(\frac{\partial Q_c}{\partial T_{c,ave}} U_{T_{c,ave}}\right)^2} \tag{B.37}$$

Where

$$\frac{\partial Q_c}{\partial \dot{m}} = C_{p,c}\, T_{c,ave} = \frac{Q_c}{\dot{m}} \tag{B.38}$$

$$\frac{\partial Q_c}{\partial T_{c,ave}} = \dot{m}\, C_{p,c} = \frac{Q_c}{T_{c,ave}} \tag{B.39}$$

From equations B.38 and B.39 and re-arranging equation B.37, hence the relative uncertainty of Q_c is determined as:

$$\frac{U_{Q_c}}{Q_c} = \pm \sqrt{\left(\frac{U_{\dot{m}}}{\dot{m}}\right)^2 + \left(\frac{U_{T_{c,ave}}}{T_{c,ave}}\right)^2} \tag{B.40}$$

Here,

$$\frac{U_{T_{c,ave}}}{T_{c,ave}} = \pm \sqrt{\left(\frac{U_{T_{c,in}}}{T_{c,in}}\right)^2 + \left(\frac{U_{T_{c,o}}}{T_{c,o}}\right)^2} \tag{B.41}$$

$$= \pm \sqrt{\left(\frac{0.25}{37.25}\right)^2 + \left(\frac{0.257}{38.85}\right)^2} = \pm 1.4142\% \tag{B.42}$$

Substitute the above equation in equation B.40 gives:

$$\frac{U_{Q_c}}{Q_c} = \pm\sqrt{\left(\frac{0.010785}{0.2157}\right)^2 + \left(\frac{0.01542}{1.4}\right)^2} = \pm 5\% \qquad \text{(B. 43)}$$

B.8 Uncertainty in Nusselt number

The average Nusselt number can be expressed as:

$$Nu = \frac{Q_{ave}\, D_h}{k_c A_s (T_{s,av} - T_{c,av})} \qquad \text{(B. 44)}$$

The uncertainty in Nusselt number is determined as:

$$U_{Nu} = \pm \sqrt{\begin{matrix}\left(\frac{\partial Nu_{av}}{\partial Q_{ave}} U_{Q_{ave}}\right)^2 + \left(\frac{\partial Nu_{av}}{\partial D_h} U_{D_h}\right)^2 + \left(\frac{\partial Nu_{av}}{\partial A_s} U_{A_s}\right)^2 \\ + \left(\frac{\partial Nu_{av}}{\partial T_{s\ ave}} U_{T_{s\ ave}}\right)^2 + \left(\frac{\partial Nu_{av}}{\partial T_{c,ave}} U_{T_{c,ave}}\right)^2\end{matrix}} \qquad \text{(B. 45)}$$

Where

$$\frac{\partial Nu}{\partial Q_{ave}} = \frac{D_h}{k_c A_s (T_{s.ave} - T_{c,ave})} = \frac{Nu}{Q_{ave}} \qquad \text{(B. 46)}$$

$$\frac{\partial Nu}{\partial D_h} = \frac{Q_{ave}}{k_c A_s (T_{s.ave} - T_{c,ave})} = \frac{Nu}{D_h} \qquad \text{(B. 47)}$$

$$\frac{\partial Nu}{\partial A_s} = \frac{-Q_{ave} D_h}{k_f {A_s}^2 (T_{s.ave} - T_{bc.ave})} = \frac{-Nu}{A_s} \qquad \text{(B. 48)}$$

$$\frac{\partial Nu}{\partial T_{s,ave}} = \frac{-Q_{ave} D_h}{k_c A_s (T_{s.ave} - T_{c.ave})^2} = \frac{-Nu}{(T_{s.ave} - T_{c,ave})} \qquad \text{(B. 49)}$$

$$\frac{\partial Nu}{\partial T_{c,in}} = \frac{Q_{ave} D_h}{k_c A_s (T_{s.ave} - T_{c,ave})^2} = \frac{Nu}{(T_{s.ave} - T_{c,ave})} \qquad \text{(B. 50)}$$

Re-arranging equation B.45, the relative uncertainty of Nusselt number is given as:

$$\frac{U_{Nu}}{Nu} = \pm \sqrt{\begin{matrix}\left(\frac{U_{Q_{ave}}}{Q_{ave}}\right)^2 + \left(\frac{U_{D_h}}{D_h}\right)^2 + \left(\frac{-U_{A_s}}{A_s}\right)^2 \\ + \left(\frac{-U_{T_{s.ave}}}{T_{s.ave} - T_{c.ave}}\right)^2 + \left(\frac{-U_{T_{c.ave}}}{T_{s.ave} - T_{c.ave}}\right)^2\end{matrix}} \qquad (B.51)$$

Where

$$\frac{U_{T_{c.ave}}}{T_{c.ave}} = \pm \sqrt{\left(\frac{U_{T_{c\,in}}}{T_{c,in}}\right)^2 + \left(\frac{U_{T_{c,o}}}{T_{c,o}}\right)^2}$$

$$= \pm \sqrt{\left(\frac{0.2}{37.25}\right)^2 + \left(\frac{0.2}{38.85}\right)^2} = \pm 1.101\% \qquad (B.52)$$

Equation B.51 becomes as follows:

$$\frac{U_{Nu}}{Nu} = \pm \sqrt{\begin{matrix}\left(\frac{5.1}{22.234}\right)^2 + \left(\frac{0.141}{23}\right)^2 + \left(\frac{-5}{29.83}\right)^2 \\ + \left(\frac{-0.2}{44.42 - 38.05}\right)^2 + \left(\frac{-0.283}{44.42 - 38.05}\right)^2\end{matrix}}$$

$$= 6.3\% \qquad (B.53)$$

الخلاصة

تعتبر المبادلات الحرارية من أهم التطبيقات الهندسية التي تستخدم لنقل الحرارة بين مائعين لهما درجات حرارة مختلفة للحصول على انتقال الحرارة بينهما دون خلط. يزداد انتقال الحرارة بزيادة الفرق بين درجات الحرارة للموائع المستخدمة. هنالك العديد من التطبيقات التي تستخدم المبادلات الحرارية مثل صناعة الأغذية وتكييف الهواء وصناعة النفط والمحطات الكهربائية. تهدف هذه الدراسة إلى تحسين أداء المبادلات الحرارية باستخدام الرغوة المعدنية وطرق توزيعها ضمن منطقة الجريان الحلقي. تمت دراسة تأثير تكوين وترتيب الرغوات المعدنية النحاسية المركبة على السطح الخارجي للأنبوب الداخلي لمبادل حراري مزدوج التدفق المعاكس بشكل تجريبي. يتكون قسم الاختبار من أنبوبين متحد المركز ؛ الأنبوب الداخلي المصنوع من النحاس والأنبوب الخارجي المصنوع من مادة PVC. تم استخدام رغوة معدنية ذات مسام لكل بوصة تساوي 15 (PPI15) ومسامية (0.95). تم استخدام الهواء كمائع عامل في كلا الجانبين الساخن والبارد. تمت تغطية مجموعة واسعة من معدل تدفق الهواء البارد ، وهي ؛ (3 ، 6 ، 12 ، 18 ، 24 ، 30 ، 36) متر مكعب / ساعة وهو ما يتوافق مع نطاق رقم رينولد من 2811 إلى 31335 ، بينما بقي معدل تدفق الهواء الساخن ثابتًا عند 3 متر مكعب / ساعة. تم اعتماد فرق درجة الحرارة بين الهواء الساخن الداخل والهواء البارد الداخل ليكون (20 درجة مئوية ، 30 درجة مئوية ، 40 درجة مئوية ، 50 درجة مئوية). أوضحت النتائج أن كمية الحرارة المنتقلة وهبوط الضغط والفعالية تعتمد على ترتيب وتكوين الرغوة المعدنية. كذلك فان أداء المبادل الحراري مع الرغوة المعدنية لجميع الترتيبات هو الأفضل مقارنة بالمبادل الحراري السلس ومعامل الاحتكاك يتناقص مع زيادة عدد رينولدز. كما أظهرت النتائج أن أفضل قيمة لمعايير تقييم الأداء هي (1.62) للحالة (7) عند رقم رينولدز (2811).

جمهوريـــــــــــة العـــــــراق
وزارة التعليم العـالي والبحث العلمي
جامـعـة الأنبـار – كـلـيـة الهـنـدسة
قســـــم الهندســـــة الميكانيكيـــــة

UNIVERSITY OF ANBAR

الأداء الهيدروليكي - الحراري لمبادل حراري مزدوج الانبوب مملوء بحلقات الرغوة المعدنية

رسالة مقدمة إلى مجلس
كـلـيـة الهـنـدسة - جامـعـة الأنبـار
وهي جزء من متطلبات نيل درجة الماجستير
في علوم الهندسة الميكانيكية

من قِبل

ثائر حميد فرحان

(بكالوريوس هندسة ميكانيكية – 1999)

بإشراف

أ.م.د. عبيد طلك فاضل

أ.م.د. حمدي عماد الدين أحمد

1442 2021